INTERNATIONAL ATOMIC ENERGY AGENCY
UNITED NATIONS EDUCATIONAL, SCIENTIFIC AND CULTURAL ORGANIZATION
INTERNATIONAL CENTRE FOR THEORETICAL PHYSICS
I.C.T.P., P.O. BOX 586, 34100 TRIESTE, ITALY, CABLE CENTRATOM TRIESTE

SMR. 758 - 44

SPRING COLLEGE IN CONDENSED MATTER
ON QUANTUM PHASES
(3 May - 10 June 1994)

==========

THE QUANTUM HALL EFFECT: NUMERICAL METHODS

John CHALKER
Department of Theoretical Physics
University of Oxford
1 Keble Road
Oxford, OX1 3NP, U.K.

==========

These are preliminary lecture notes, intended only for distribution to participants.

==========

Notes for Lectures 1–4

John Chalker

In: "Symmetry & Structural Properties of Condensed Matter"
Eds W. Florek, D. Lipiński & T. Lulek
(World Scientific, 1993)

Anderson Localisation and the Integer Quantum Hall Effect

J T Chalker

Theoretical Physics, University of Oxford, 1 Keble Road, Oxford, OX1 3NP, United Kingdom

Abstract

A brief review is presented of the role played by Anderson localisation in the integer quantum Hall effect. Particular emphasis is placed on recent experimental and numerical studies of transitions between states with different quantised values of the Hall conductivity. These transitions are critical points at which there is a divergent length scale: the localisation length. A summary is given of universal features at and near the critical points.

NB/C

This summary was written two years ago and for a more general audience than the participants at this summer school. It is intended as an outline of the main points.

1 Introduction

The existence of the integer quantum Hall effect is intimately bound up with Anderson localisation. Although this fact was appreciated [1] rather quickly after von Klitzing's [2] discovery, initial theoretical work concentrated on a different aspect: the exactness with which the Hall conductivity is quantised. By contrast, in recent years there has been a considerable effort to study the quantum Hall effect as a localisation phenomenon. Work has focussed on behaviour which is likely to be universal, in the sense that it is independent of details of the experimental sample or theoretical model. Such universality is expected in the vicinity of transitions between different quantum Hall plateaus, on the grounds that these transitions are analogous to continuous phase transitions in statistical mechanical systems. In this article we present a brief review of progress in the area.

We begin with an outline of some experimental facts, and of the role played by Anderson localisation in their interpretation. (An extensive review can be found, for example, in the book edited by Prange and Girvin [3]). The integer quantum Hall effect is observed in a two-dimensional electron gas (produced at a semiconductor interface) at low temperature and subject to a strong, perpendicular magnetic field. The electron gas is probed by measuring its conductivity tensor, σ. The Hall conductivity, σ_{xy}, regarded as a function of electron density, n, (or, equivalently, the inverse, $1/B$, of the magnetic field strength), has the form of a staircase, consisting of broad plateaus at integer multiples of e^2/h (with e the electron charge and h Planck's constant), separated by narrow risers. The dissipative conductivity, σ_{xx}, is very small at electron densities for which the Hall conductivity is quantised, but has dramatic Shubnikov - de Haas peaks which coincide with the risers in σ_{xy} (Fig 1). Both the transitions between Hall plateaus and the Shubnikov - de Haas peaks become sharper at lower temperatures, as indicated schematically in Fig 2.

This temperature dependence is very interesting from a theoretical viewpoint, because one of the principal consequences of reducing temperature is presumably to increase the inelastic scattering length for electrons near the Fermi energy. We can therefore regard the evolution of σ, with decreasing temperature, as an evolution with increasing length scale. Applying standard scaling ideas, one expects universal behaviour at sufficiently large scales. This means, in particular, that provided σ is an appropriate scaling variable, its flow should be determined only by its initial value, and not by other characteristics of the sample. Kheml'nitskii [4] has proposed a scaling flow diagram for such evolution, in which the variation of σ with increasing length scale, at fixed electron density, is represented by a trajectory on the $\sigma_{xy} - \sigma_{xx}$ plane. A collection of trajectories, each corresponding to a different electron density, provides an alternative way of presenting the type of data depicted in Fig 2. An extensive experimental study is described on these lines in Ref [5].

The structure of the resulting flow diagram, which is shown in Fig 3, is largely determined by two sets of fixed points. Attractive fixed points, at $(\sigma_{xy}, \sigma_{xx}) = (Ne^2/h, 0)$, with N integer, are associated with behaviour in Hall plateaus. Delocalisation fixed points (the motivation for this terminology will become evident below) control transitions between plateaus and are situated at $(\sigma_{xy}, \sigma_{xx}) = ([N + 1/2]e^2/h, \sigma^*)$, with σ^* a constant. Flow in the vicinity of these latter points is attractive for deviations in the σ_{xx} direction, but repulsive for deviations in the σ_{xy} direction. As a result, almost all trajectories arrive at a stable fixed point in the low temperature limit. Correspondingly, the Hall conductivity is quantised for almost all electron densities, and transitions between quantised values (as a function of electron density) are abrupt. The exceptional trajectories end at delocalisation fixed points; they are responsible for Shubnikov - de Haas peaks, which are thus expected to have vanishing width at zero temperature. At a low but non-zero temperature, a small fraction of trajectories remain in the vicinity of the delocalisation fixed point, and both the transitions between Hall plateaus and

the Shubnikov - de Haas peaks retain a finite width (in n or $1/B$).

The experiments and numerical calculations that we describe in subsequent sections are specifically concerned with two features of this scaling diagram: the flow away from the delocalisation fixed points, as charcterised by a critical exponent, ν, and the position of these fixed points, represented by the value of σ^*.

It is clearly important to supplement the phenomenological scaling description with a microscopic picture. We shall do so within a single-particle framework; neglect of many-body correlations excludes, in particular, any discussion of the fractional quantum Hall effect. The spectrum for a charged particle moving in two dimensions in a perpendicular magnetic field consists of a series of macroscopically degenerate Landau levels. A more realistic model of the experimental system should include scattering from impurities and inhomogeneities within the sample, which lifts the degeneracy and broadens the Landau levels. Provided the magnetic field is strong enough, however, the disorder-broadening is less than the cyclotron energy, and the levels retain their identity. It turns out that the states within each disorder-broadened Landau level fall into two categories, for reasons that we shall outline heuristically in Sec 2. States in the tails of Landau levels are Anderson localised, meaning that each is trapped within a particular, microscopic region of the system. By contrast, states near the centre of each Landau level have wavefunctions that extend throughout that sample. The distinction is crucial for the conductivity, since, within linear response, a constant external electric field cannot induce transitions between different localised states. Thus, only those electrons occupying extended states participate in current flow. Indeed, given these features of the eignestates, one can deduce the essentials in the dependence of conductivity on electron density. To do so imagine adding electrons at zero temperature to a system with the spectrum sketched in Fig 4. Initially, all occupied states are localised and transport is impossible. Addition of more electrons brings the Fermi energy into a region

of extended states, so that σ_{xy} increases with n. In this situation, σ_{xx} is non-zero, because inelastic scattering of electrons close to the Fermi energy gives rise to dissipation. A further increase in n brings the Fermi energy into the localised states in the upper tail of the Landau level. Now, a variation in electron density does not alter the number of extended, current-carrying states that are occupied. Correspondingly, the Hall conductivity exhibits a plateau. Also, since the occupied, current-carrying states are buried at some depth beneath the Fermi energy, dissipation is necessarily activated, and vanishes in the low temperature limit. In turn, this implies that the Hall angle is 90°, and thus that $\sigma_{xx} = 0$. The sequence is repeated on moving the Fermi energy through higher Landau levels, and generates the behaviour represented in Fig 1.

To understand the temperature dependence of σ in this way, one needs a more detailed characterisation of the localised states. This is provided by the (energy-dependent) localisation length, ξ, which is a measure of their size. the localisation length is small in the tails of Landau levels, and infinite at energies where states are extended. There is, in fact, extensive numerical evidence (which we cite in Sec 4), that ξ diverges only at one energy within each disorder-broadened Landau level. Near this critical energy, E_c, ξ is believed to have a power-law dependence on energy, E :

$$\xi \sim |E - E_c|^{-\nu}.$$

It follows, in principle, that extended states constitute a vanishing fraction of the spectrum in the thermodynamic limit. More realistically, one expects some cut-off to intervene. One candidate, at non-zero temperature, is the inelastic scattering length; an alternative is simply the system size. In either case, localisation on scales larger than the cut-off is physically irrelevant. There exists a window in energy (as illustrated in Fig 5), within which ξ is greater than the cut-off and states are effectively extended. The width of this window, expressed via the electron density, determines the width of risers in

σ_{xy} and of Shubnikov - de Haas peaks in σ_{xx}. It is apparent that both will become narrower as the cutt-off increases, and hence that this microscopic description is consistent with the scaling flow diagram.

2 Localisation and Percolation

There is an intuitively appealing picture of Anderson localisation in the context of the integer quantum Hall effect, which relates localisation to classical percolation. The relevant ideas have been developed by a number of authors [6]. Their starting point is to consider electrons moving in a disordered potential, $V(r)$, which varies only on a lengthscale, λ, much larger than the magnetic length, l_c. In this limit, there are two components to electron motion, which have widely separated timescales: rapid cyclotron orbiting, and slow drift of the orbit guiding center. The essential simplifying feature is that guiding centres drift along equipotentials of $V(r)$. From this it is argued that each eigenstate has its probability density concentrated on a strip of width l_c around one connected contour of $V(r)$. The energy of an eigenstate is the sum of the kinetic energy of cyclotron motion, $(N + 1/2)\hbar\omega_c$, and the potential energy of the contour with which the state is associated. By this reasoning, there are extended eigenstates at energy $(N + 1/2)\hbar\omega + V_0$ if the equipotentials of $V(r)$ at energy V_0 percolate. It is expected very generally that equipotentials of a random potential percolate only at one energy, and hence that extended eigenstates are found at a unique energy within each disorder-broadened Landau level. Classical percolation theory leads, in addition, to the prediction [6] that the localisation length exponent should take the value $\nu = 4/3$.

The shortcomings of this description are the neglect of quantum tunnelling between different portions of contour at a given energy, and of interference between waves that have tunnelled via different routes. Both these are included in the network model [7], discussed in Sec 4. We shall see that, although clas-

sical ideas lead to the correct qualitative behaviour, quantitative predictions for ν are incorrect.

3 Experimental Measurement of ν

There have been two detailed experimental studies of the critical behaviour associated with the delocalisation fixed points in the scaling flow diagram (Fig 3).

The first, by Tsui and co-workers [8], used, as a cut-off, the inelastic scattering length, l_{in}, and involved measurements of the width, in $1/B$, of transitions between Hall plateaus and of Shubnikov - de Haas peaks. This width is proportional to the width in energy of the window over which $\xi \geq l_c$ (see Fig 5). The inelastic scattering length is expected to diverge with a power law as temperature, T, is reduced:

$$l_{in} \sim T^{-p/2}$$

(the notation $p/2$ for the power being simply a convention). Combining this with a power law divergence of the localisation length [8], one expects the width of transitions to vary as

$$\Delta(1/B) \sim T^{\kappa}$$

with

$$\kappa = \frac{p}{2\nu}.$$

Such behaviour is indeed observed [8], with $\kappa = 0.42$.

The principal difficulty involved in comparing these measurements with theoretical results is that, while the value of ν can be determined with reasonble confidence from the numerical simulations described in Sec 4, the value of p is dependent on the dominant inelastic scattering mechanism and quite uncertain.

An elegant approach due to Koch *et al* [9] avoids these problems by constructing samples sufficiently small that l_{in} exceeds the sample size, l_s, at low temperature. As a result, the measured width of transitions in the low temperature limit is expected to be

$$\Delta(1/B) \sim l_s^{-1/\nu}.$$

Measurements on a sequence of samples with l_s in the range $8 - 64\ \mu m$ yields $\nu = 2.3 \pm 0.1$, a value which is in disagreement with the results of classical percolation theory, but, as we shall see in Sec 4, is in striking agreement with numerical simulations.

4 Numerical Calculation of ν

There is a reassuring level of accord, both between different numerical calculations of the localisation length exponent, ν, and between these calculations and the experiments outlined in the previous section. It is perhaps worth stressing that, in this respect, localisation in the context of the quantum Hall effect is unique. For example, at the mobility edge in three dimensional systems without a magnetic field, the localisation length exponent is measured to be $\nu = 0.5$ or $\nu = 1$, depending on the material, while results of simulation range from $\nu = 1.1$ to $\nu = 1.5$ [10].

A necessary initial step in all numerical calculations in this area is to discretise the problem. In practice, there are two ways of doing this. The first is to project the Hamiltonian onto the subspace spanned by states from a single Landau level. The number of basis states is then proportional to the area of the system considered, measured in units of l_c^2. Alternatively, one can start from the picture described in Sec 2, in which a cyclotron guiding centre drifts along contours of the potential. Adding quantum tunnelling across saddlepoints of the potential, one obtains the network model of Ref [7]. In this case, the number of independent degrees of freedom invloved is

given by the area of the system, measured in units of the correlation length, λ, of the disordered potential.

The most important quantity characterising any model is the ratio, l_c/λ, of the magnetic length to the correlation length of the disordered potential. Experimentally, it is likely that both the limit $l_c/\lambda \ll 1$ and the limit $l_c/\lambda \gg 1$ are realised, in wide spacer-layer heterojunctions and in MOSFET's respectively. The first approach to discretisation allows both limits to be investigated (although it becomes increasingly inefficient as l_c/λ decreases), whilst the second approach is restricted to $l_c/\lambda \ll 1$.

Localisation properties in a suitably discretised model can be determined numerically, either via a finite-size scaling analysis of the behaviour on long strips [7, 11] or by diagonalisation of the Hamiltonian for a square sample [12]. Results from both methods and from both kinds of model agree (at least within the lowest Landau level), the most precise value quoted for the localisation length exponent being $\nu = 2.34 \pm 0.04$ [11].

5 Universal Dissipative Conductance

The coordinate, σ^*, of the delocalisation fixed point characterises the long-distance response of a system at a critical point. Because of this, there are good grounds [13] for expecting its value, like that of ν, to be universal.

There are two very different experimental approaches to determining σ^*. One is to measure the height of Shubnikov - de Haas peaks as the Fermi energy sweeps through the critical energy, E_c. Measurements of this type give sample-dependent results, with no evidence for universality. An alternative technique is to place the Fermi energy mid-way between two Landau levels and measure the temperature dependence of the dissipation, which is due to quasiparticles thermally excited to the extended states in the states at energy $\pm\Delta E$ either side of the Fermi energy. Simple arguments suggest activated

behaviour [14], with

$$\sigma_{xx}(T) = 2\sigma^* \exp(-\Delta E/T),$$

where the factor of 2 arises because of contributions to dissipation from both the level above the Fermi energy and the one below. Data of this kind, due to Clark *et al* [14], from a variety of samples and for a range of Landau levels, from the lowest to the tenth orbital level, yield a single value for σ^* of $0.5e^2/h$, within a precision of perhaps $\pm 10\%$. The reason for the discrepancy between the two types of experiment remains unclear.

The value of σ^* has been calculated both by resumming a series in powers of the disordered potential [15], and from numerical diagonalisation of the Hamiltonian for finite systems [16]. Results are consistent between the two calculations and with the experiments of Clark *et al.* Very recently, the value of σ^* has been compared in several models that involve different statistical assumptions about the scattering potential felt by electrons [17]. The value appears to be model independent.

If one accepts this conclusion, an interesting consequence follows for the fractional quantum Hall effect, which we mention as an aside. The quasiparticles in the fractional quantum Hall effect are believed [3] to be fractionally charged, with charge e^*, in place of the electron charge, e. Suppose that, at least at low density, these quasiparticles respond to disorder in much the same way as do electrons in the integer quantum Hall effect. A measurement of the dissipation in a sample displaying a fractionally quantised value of its Hall conductance will then have the same activated behaviour as found in the integer effect. The prefactor, σ^*, however, should take the value $0.5(e^*)^2/h$, in place of $0.5e^2/h$. Clark *et al* [14] have used this approach to measure the quasiparticle charge in several fractional states.

6 Conclusions

The quantum Hall effect is dependent for its existence on Anderson localisation, in the sense that, without localisation (or some alternative mechanism), there could be no plateaus in the Hall conductance as a function of electron density. Understanding of localisation makes no contribution to the explanation of one of the most striking features of the quantum Hall effect: the exactness of quantisation. Rather, it represents a new area of investigation. The transitions between different quantised Hall states are examples of zero-temperature quantum phase transitions, with a divergent length scale, the localisation length. Close to the transition point, universal critical behaviour is expected. In fact, there is an impressive concord on critical properties, both between simulations on different models and between these simulations and experiment.

Acknowledgements

I should like to thank the organising committee for their invitation to take part in SSPCM2, and for their hospitality in Poznan. My own work in the area covered by this review was done in collaboration with P D Coddington, G J Daniell and J G Eastmond, to whom I am grateful. This work was supported in part by SERC, under Grant No. GR/GO 2727, and in part by the European Community, under Grant No. SCC CT90 0020.

References

[1] R E Prange, Phys Rev B 23 4802 (1981); H Aoki and T Ando, Sol State Comm 38 1079 (1981).

[2] K von Klitzing, G Dorda and M Pepper, Phys Rev Lett 45 494 (1980).

[3] R E Prange and S M Girvin (Editors) *The Quantum Hall Effect*, Springer (New York) 1990.

[4] D E Khmel'nitskii Piz'ma Zh Eksp Teor Fiz **82** 454 (1983) [JETP Lett **38** 552 (1983)]; see also A M M Pruisken in Ref [3].

[5] H P Wei, D C Tsui and A M M Pruisken, Phys Rev B**33** 1488 (1986).

[6] M Tsukada, J Phys Soc Jpn **41** 1466 (1976); S V Iordansky, Sol State Comm **43** 1 (1982); R F Kazarinov and S Luryi, Phys Rev B **25** 7626 (1982); R E Prange and R Joynt, Phys Rev B **25** 2943 (1982); S A Trugman, Phys Rev B **27** 7539 (1983); B Shapiro, Phys Rev B **33** 8447 (1986).

[7] J T Chalker and P D Coddington, J Phys C **21** 2665 (1988).

[8] H P Wei, D C Tsui, M Paalanen and A M M Pruisken, Phys Rev Lett **61** 1294 (1988).

[9] S Koch, R Haug, K von Klitzing and K Ploog, Phys Rev Lett **67** 883 (1991).

[10] B Kramer and A MacKinnon, Reports on Progress in Physics (to appear).

[11] B Huckestein and B Kramer, Phys Rev Lett **64** 1437 (1990).

[12] Y Huo and R N Bhatt, Phys Rev Lett **68** 1375 (1992).

[13] M P A Fisher, G Grinstein and S M Girvin, Phys Rev Lett **64** 587 (1990)

[14] R G Clark, S R Haynes, J V Branch, J R Mallett, A M Suckling, P A Wright, P M W Oswald, J J Harris and C T Foxon, Surf Sci **229** 25 (1990).

[15] R Singh and S Chakravarty, Nucl Phys B **265** 265 (1986).

[16] J T Chalker and G J Daniel, Phys Rev Lett **61** 593 (1988).

[17] Y Hao, R E Hetzel and R N Bhatt, unpublished.

Figure Captions

Fig 1
Schematic dependence of σ_{xx} and σ_{xy} on electron density.

Fig 2
Variation with temperature of the dependence of components of σ on electron density.

Fig 3
The scaling flow diagram.

Fig 4
The density of single particle states under the conditions of the quantum Hall effect. The portions of the spectrum taken up by extended states are indicated. The remaining states are localised.

Fig 5
Dependence of localisation length on energy, within one disorder-broadened Landau level.

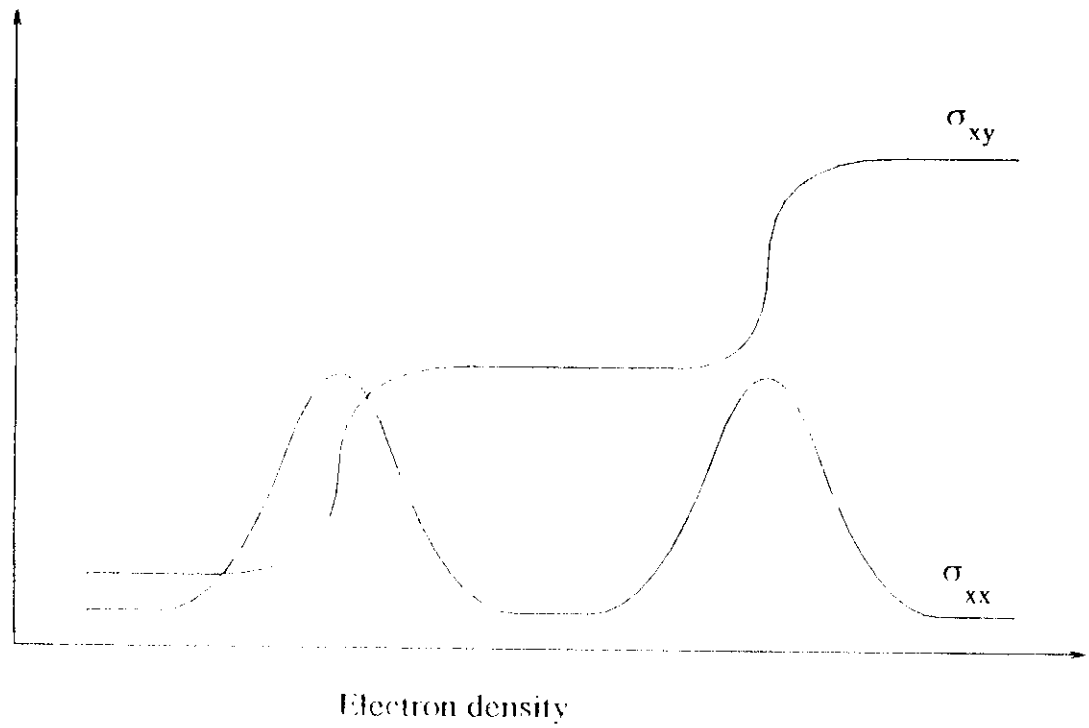

Fig 1

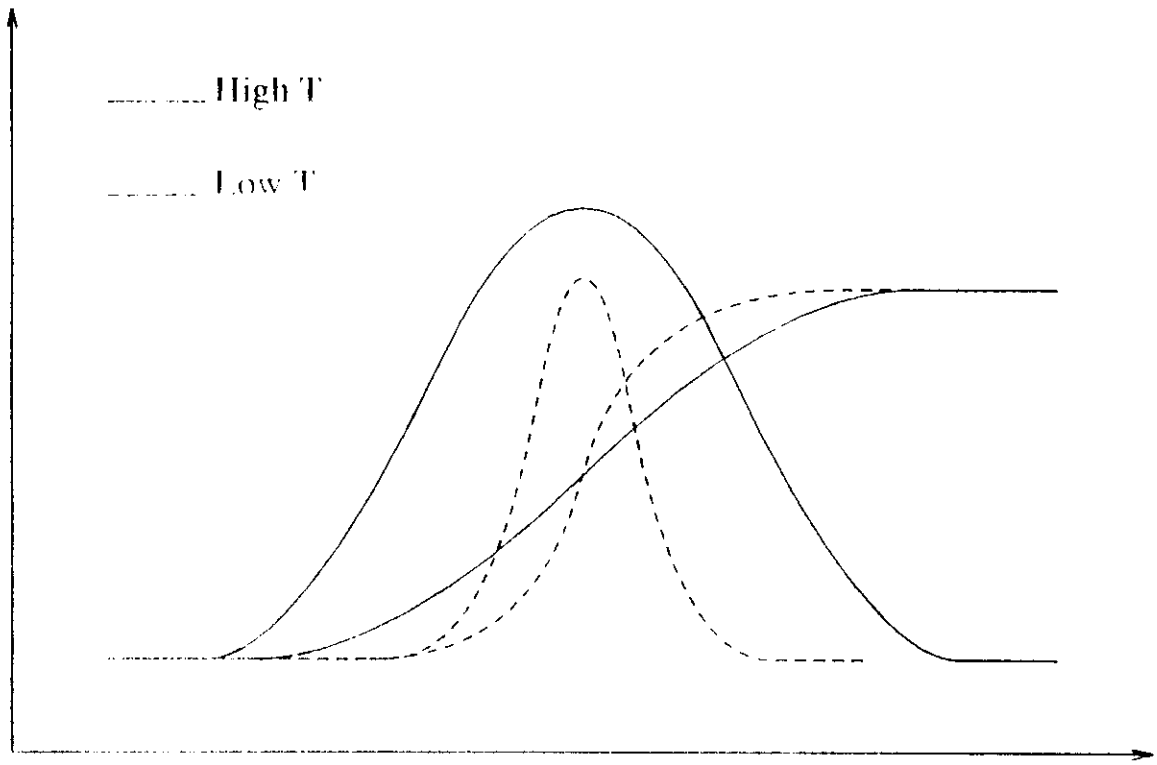

Fig 2

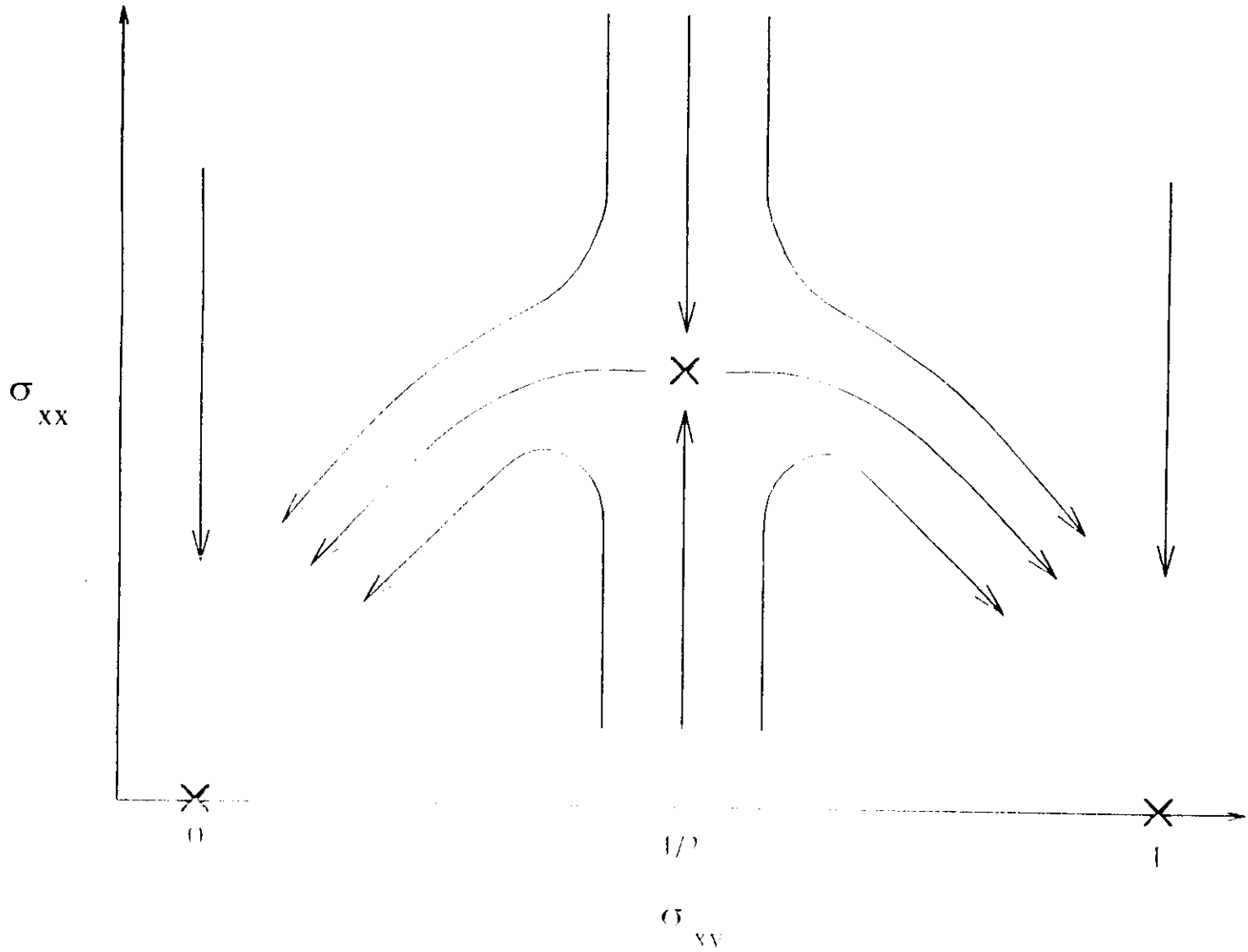

Fig 3

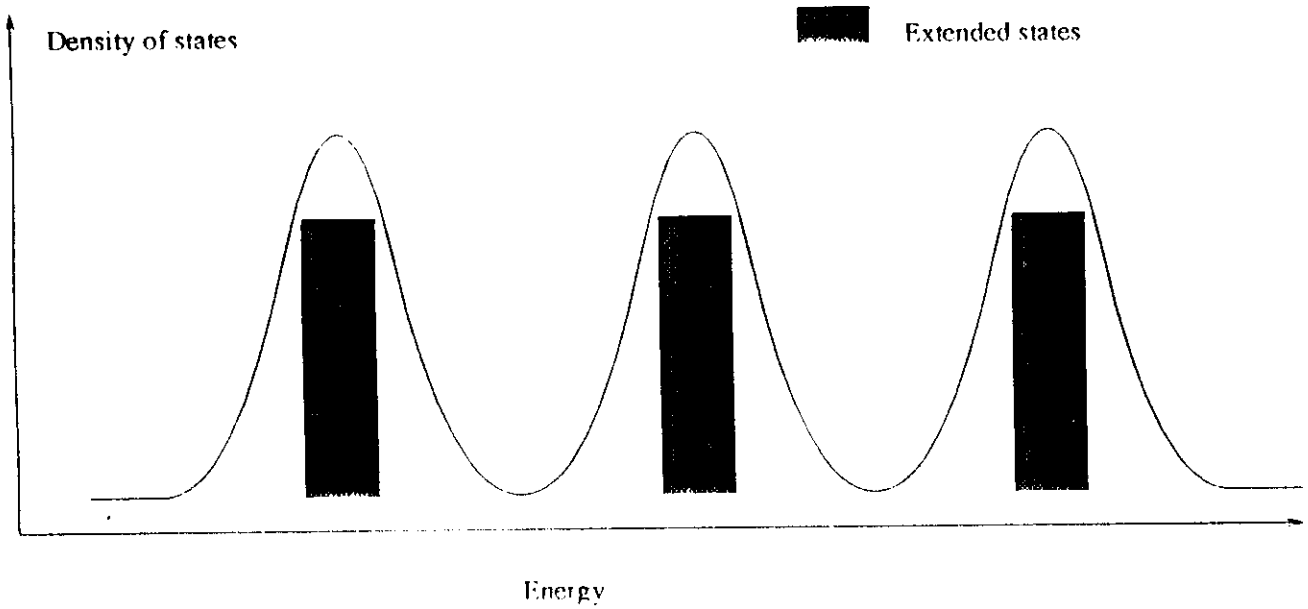

Fig 4

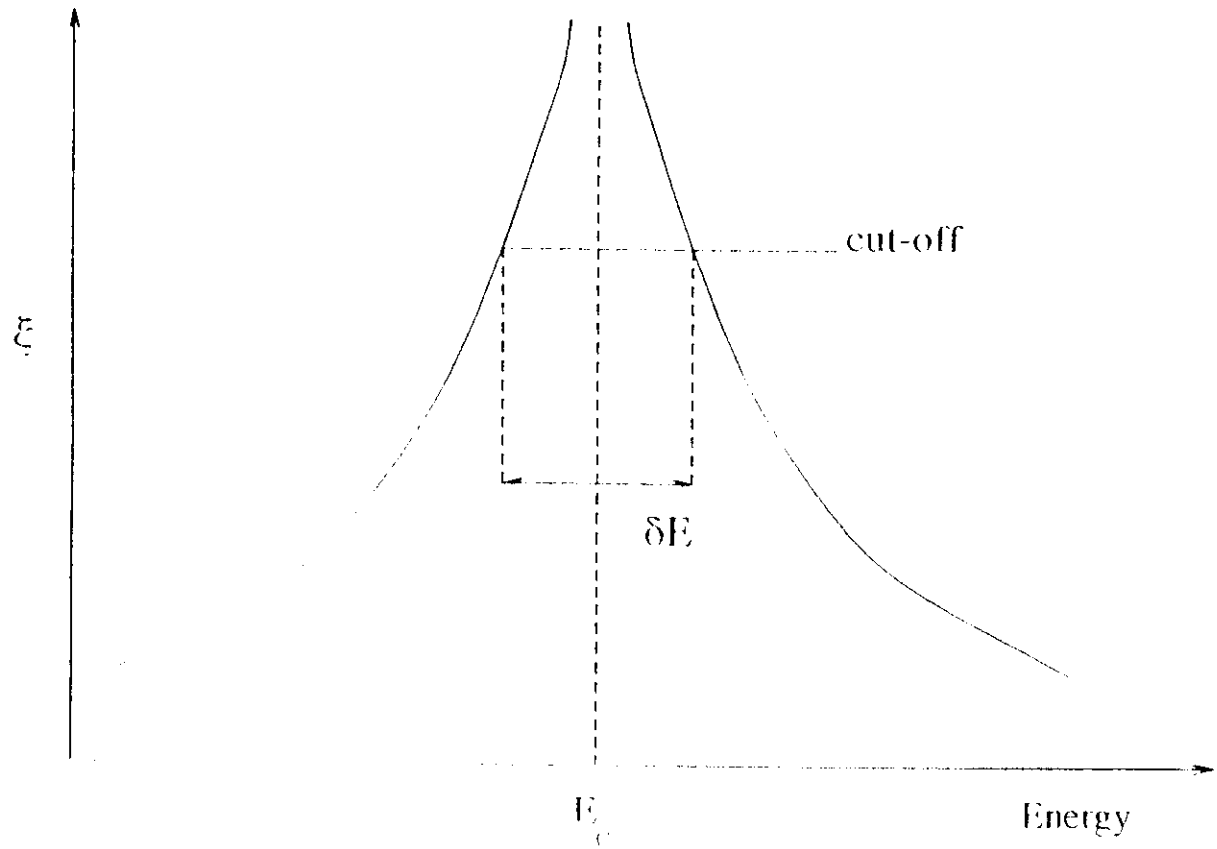

Fig 5

The Integer Quantum Hall Effect and Anderson Localisation

Overview:

① { Introduction
  Scaling at the mobility edge
    - phenomenology & experiment

②+③ { Models
  Numerical techniques & results

④ { Properties of electron states near mobility edge

2D electron gas

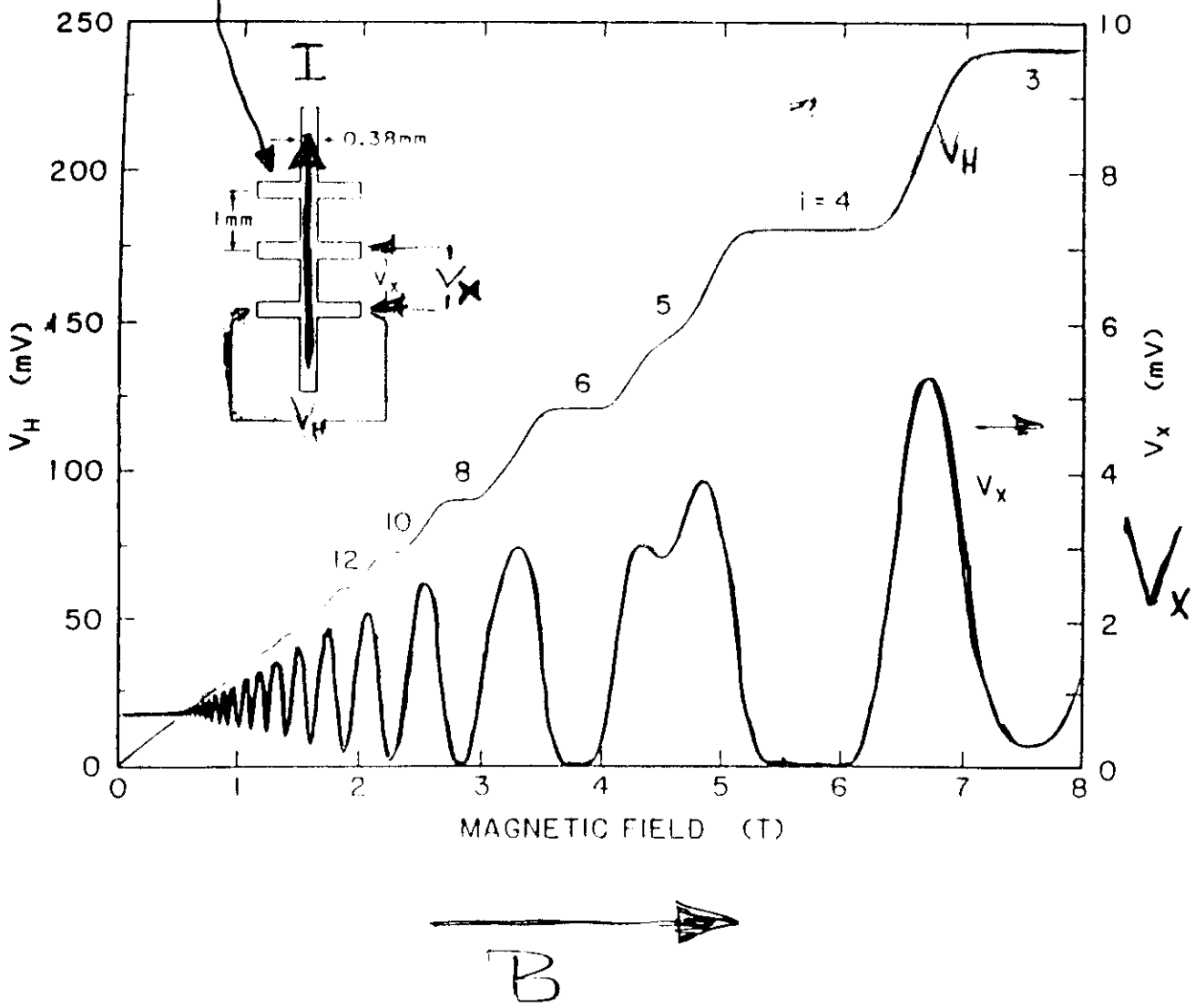

LECTURE 1

Introduction | ① Overview

Ask questions

Will talk about IQHE mainly as localisation phenomenon

Will talk almost entirely in single particle terms – many body aspects may be important but are not yet understood

-- Go through ①

② IQHE trace – the phenomenon to be understood

2DEG, low T : measure V_x, V_H vs B
oscillations in ρ_{xx}, plateaux in ρ_{xy}

Board

Density of states

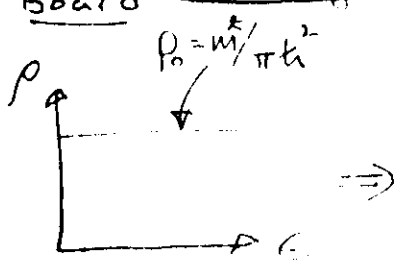

Ideal, B=0

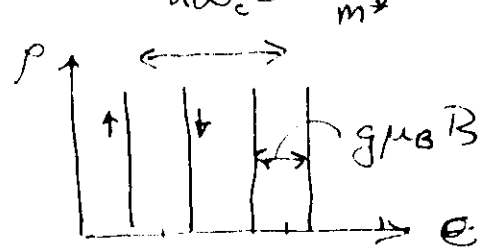

Ideal, B≠0

Free electrons $\rho_{xy} = B/ne$

States/unit area in Landau level

$\frac{1}{2}\rho_0 \hbar\omega_c$

$= \frac{1}{2\pi} \cdot \frac{eB}{\hbar} = \frac{1}{2\pi\ell_c^2}$

$\ell_c = \left(\hbar/eB\right)^{1/2}$

Increase B ⇒ sweep ϵ_F down through Landau levels

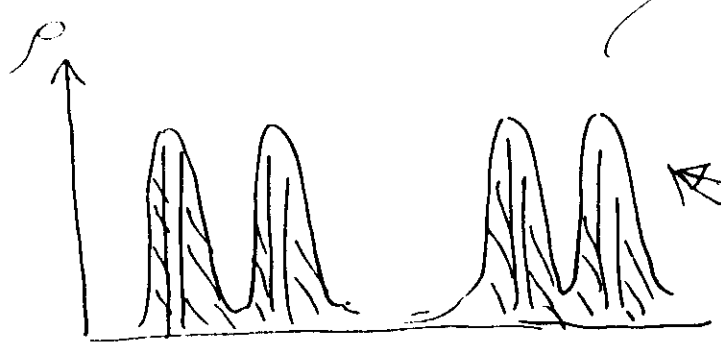

Don't rule out!

Real, B large

Mention

$\sigma_{xy} = \frac{-\rho_{xy}}{\rho_{xx}^2 + \rho_{xy}^2}$

Free electrons
$\sigma_{xy} = \frac{1}{2\pi\ell_c^2} f \frac{e}{B} = f\frac{e^2}{h}$

(3) Exactness of quantization

Why don't impurities affect σ_{xy} on plateaus?

Picture — two fluxes

$\Phi(t)$ to generate emf

Have

(1) $\frac{d\Phi}{dt} = \int d\underline{l} \cdot \underline{E} = \int d\underline{l} \cdot \rho \underline{j} = \rho_{xy} I$

Φ (if $\rho_{xx} = 0$

(2) $\Phi \to \Phi + h/e$

- eigenstates unchanged
- adiabatic flux increase transfers charge $\int I(t) dt$ along length of cylinder
- I same everywhere

$\Rightarrow \rho_{xy}$ same everywhere

NB Hall current carried by extended states buried below E_F

Localisation — Scales in problem

Magnetic field : $\hbar\omega_c$, l_c

Disorder apparently $\langle V(r)V(r')\rangle = V_0^2 f(r/\lambda)$

IQHE : $V_0/\hbar\omega_c \lesssim 1$

$\frac{l_c}{\lambda}$ ~~free~~ unrestricted

Classical Limit

$l_c \to 0$ $(B \to \infty)$

Gives plausibility argument for existence of extended

4. Percolation

Exactness of quantization

(Laughlin 81, Halperin 82 ...)

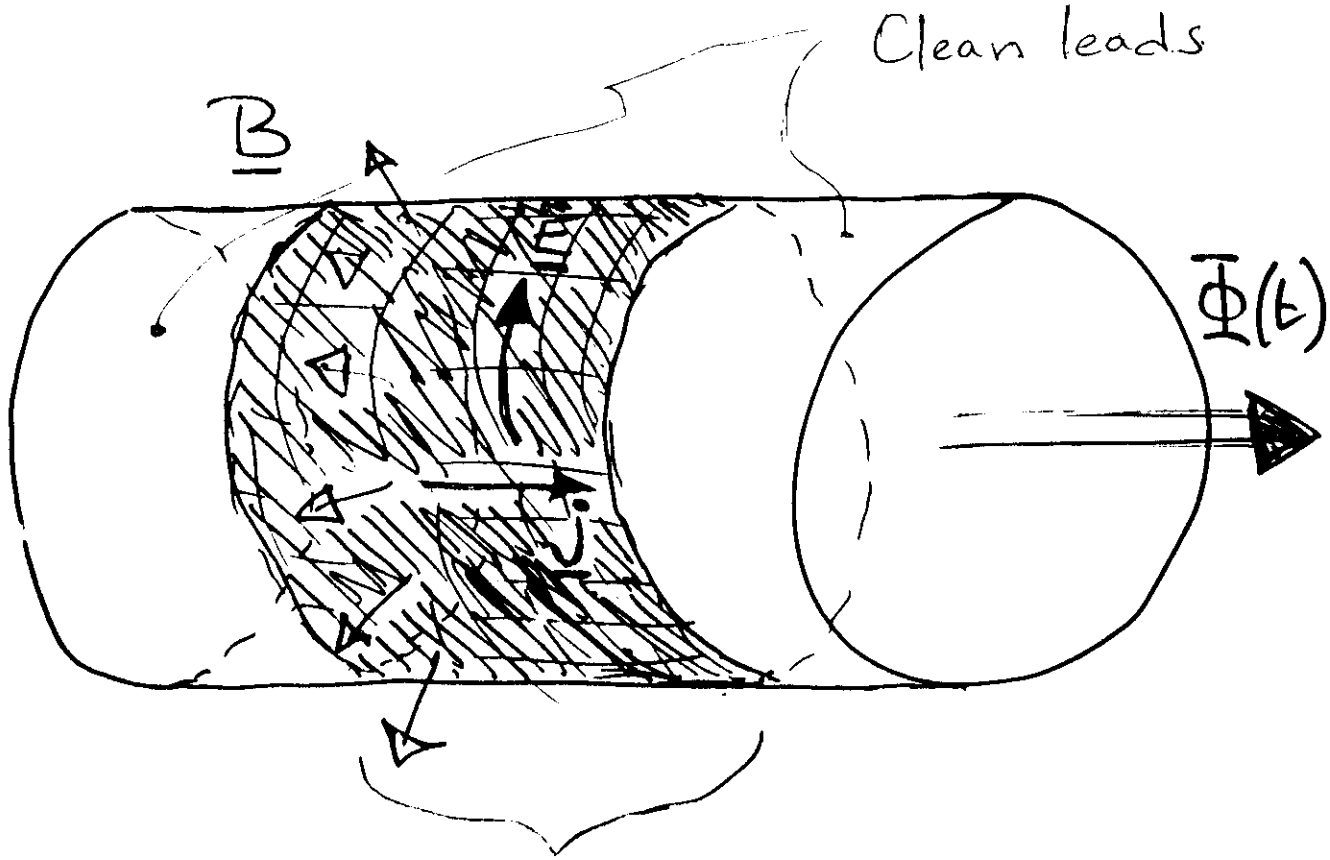

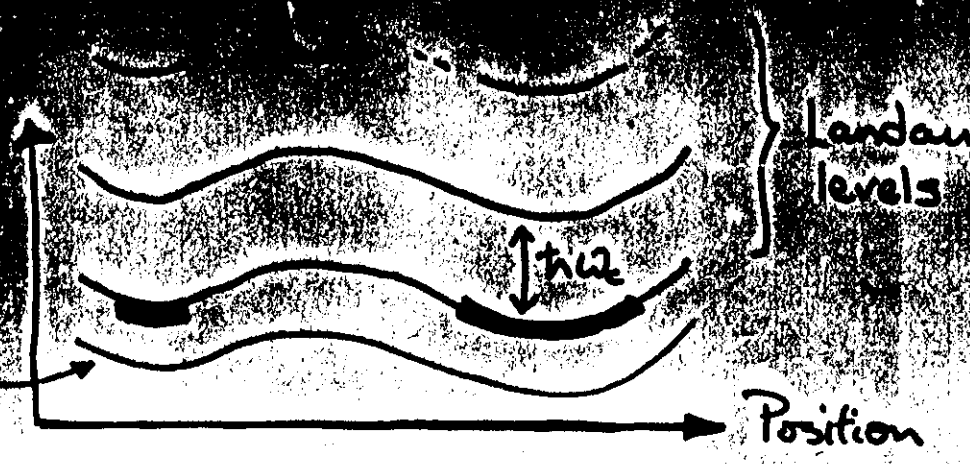
Landau levels
$\hbar\omega_c$
Position

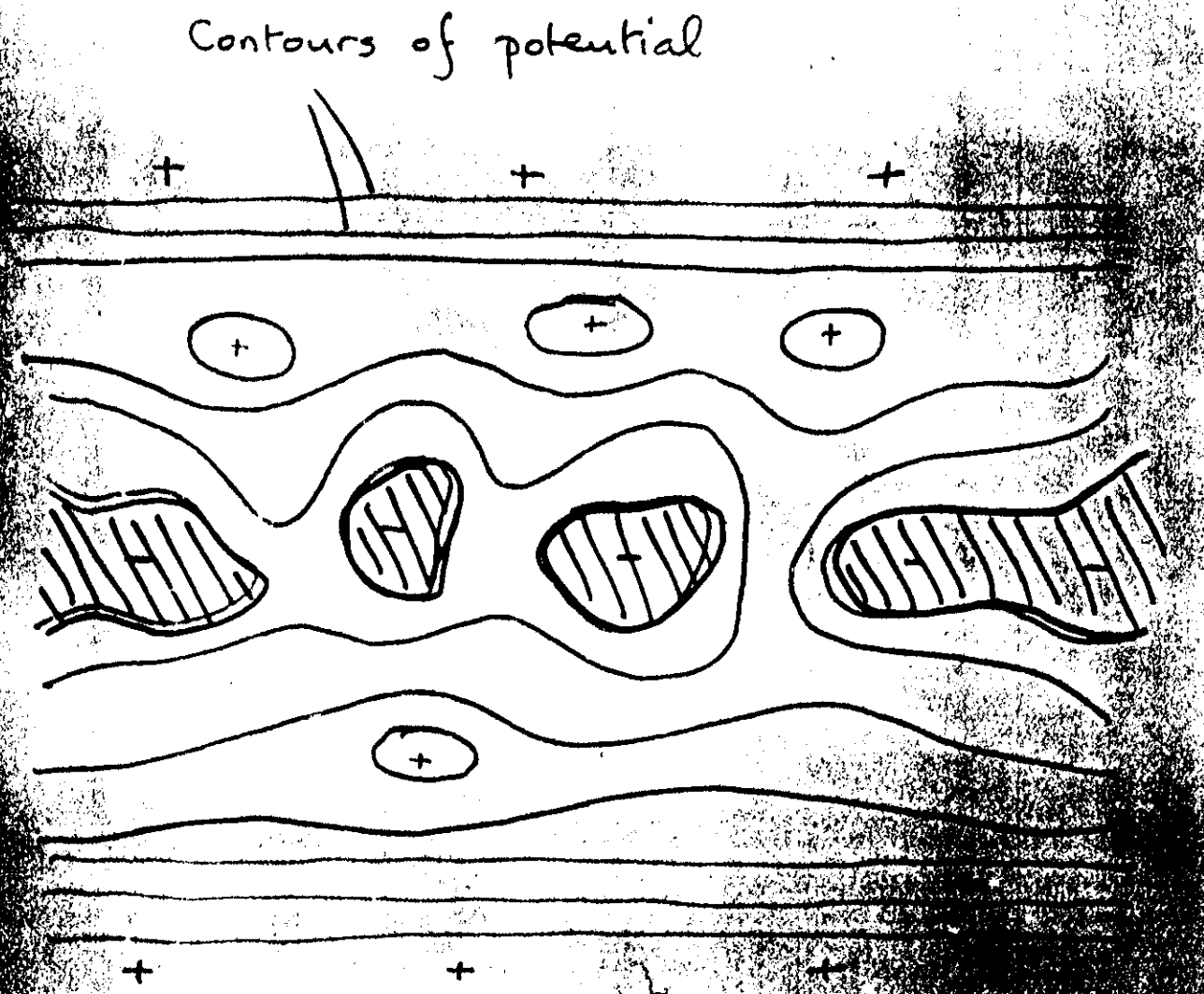
Contours of potential

Scaling theory (measure σ in units of e^2/h)

$B=0$ $\quad \dfrac{d\,\sigma(L)}{d\,\ln\{L\}} = f(\sigma(L))$

weak localisation theory ($\sigma \gg 1$)

$f \sim \begin{cases} -2/\pi & (B=0) \\ -\dfrac{1}{2\pi^2}\,\dfrac{1}{\sigma} & (B \text{ weak}) \end{cases}$

$\Rightarrow$ much larger localisation length if σ large, but no extended states

Pruisken 83 $\quad \sigma_{xx}$ and σ_{xy} coupling constants in effective field theory

σ_{xy} appears as $\exp(2\pi i\, \sigma_{xy} \times \text{integer})$

$$\begin{cases} \dfrac{d\,\sigma_{xx}(L)}{d\,\ln L} = f_{xx}[\sigma(L)] & f_{xx}\left(\sigma_{xx}(L), \sigma_{xy}(L)\right) \\ \dfrac{d\,\sigma_{xy}(L)}{d\,\ln L} = f_{xy}[\sigma(L)] & f_{xy}(\text{"bilinear"}) \end{cases}$$

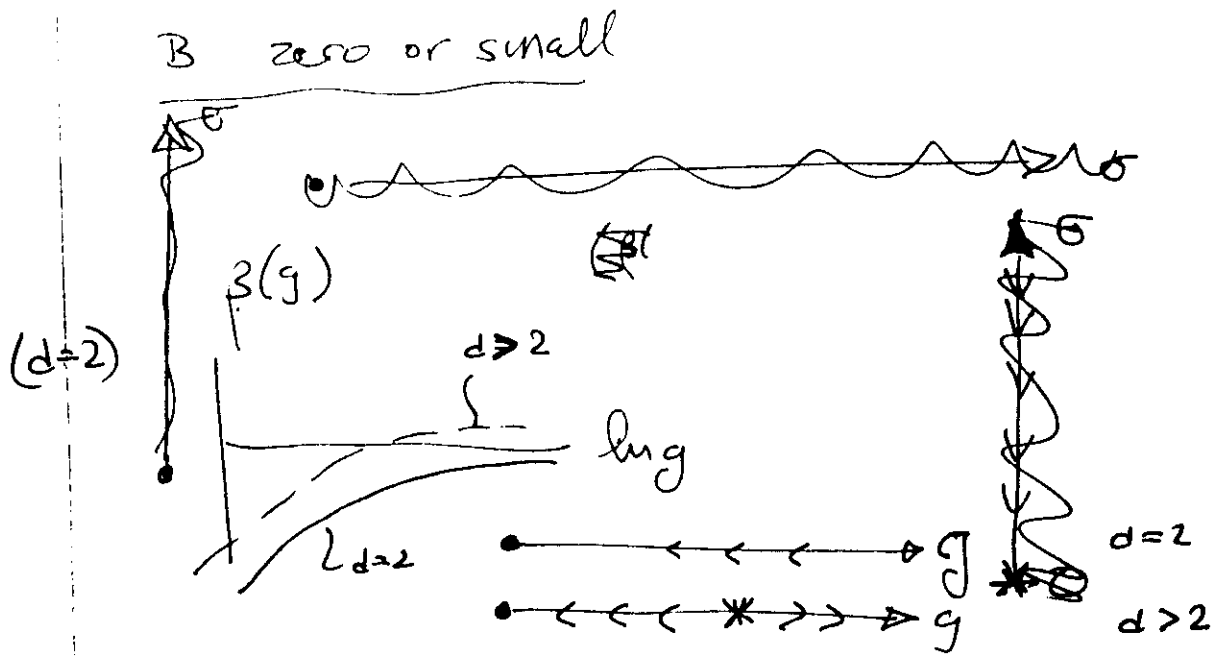

Scaling in integer quantum Hall effect

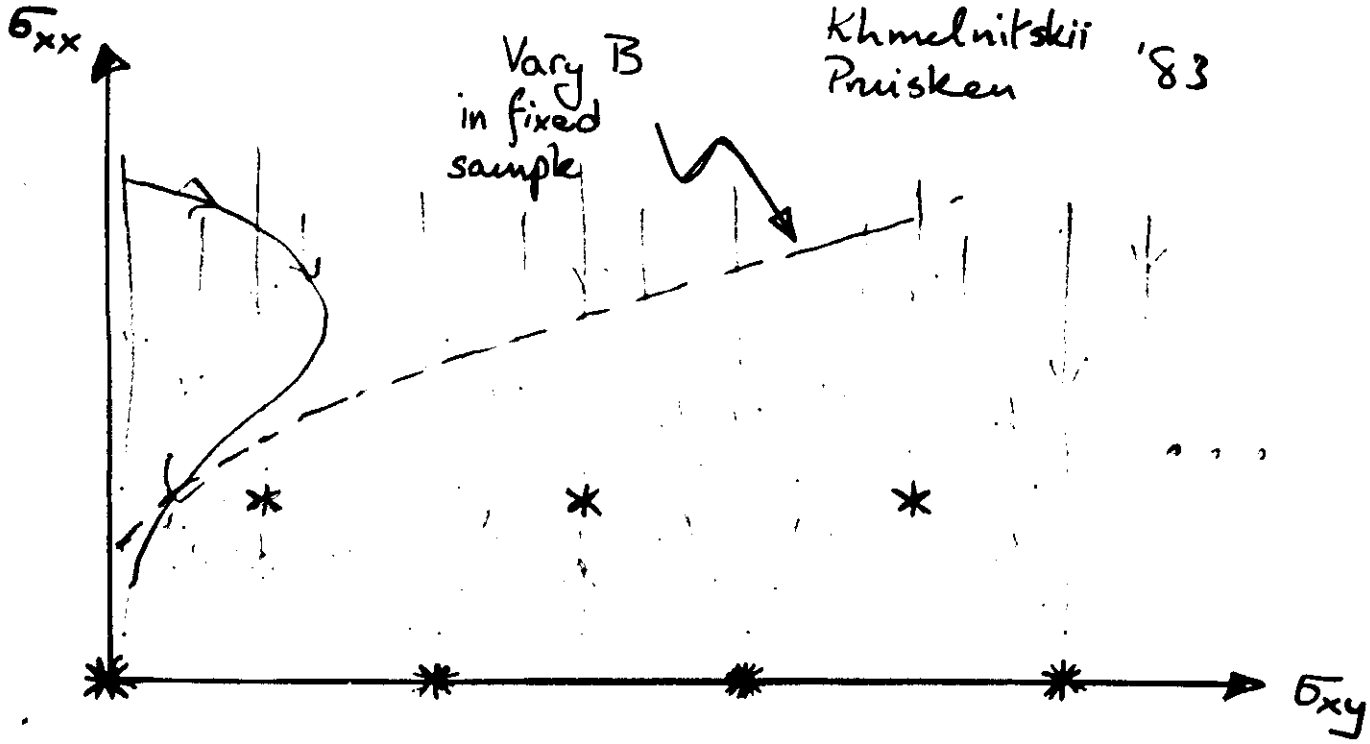

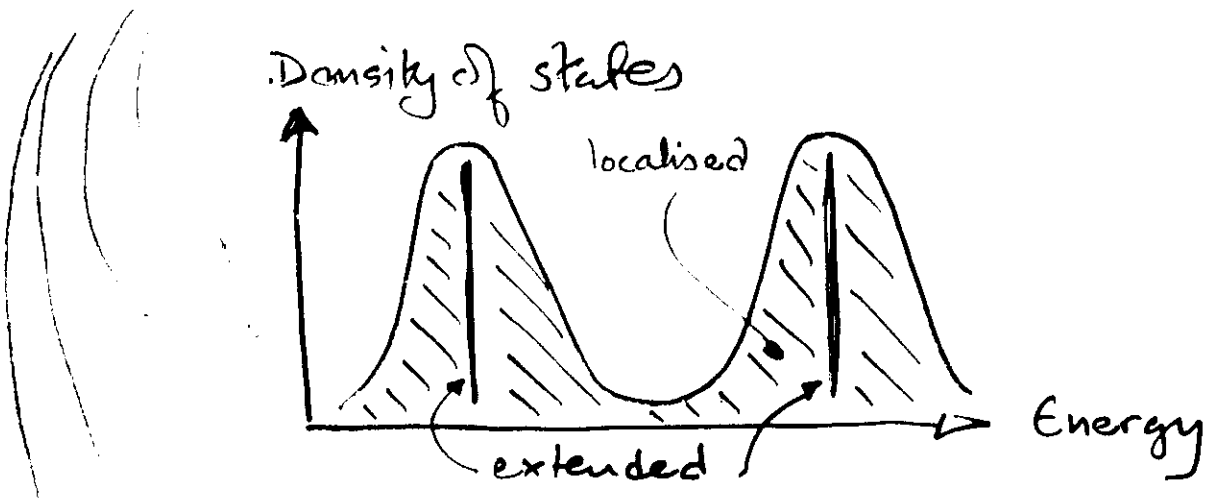

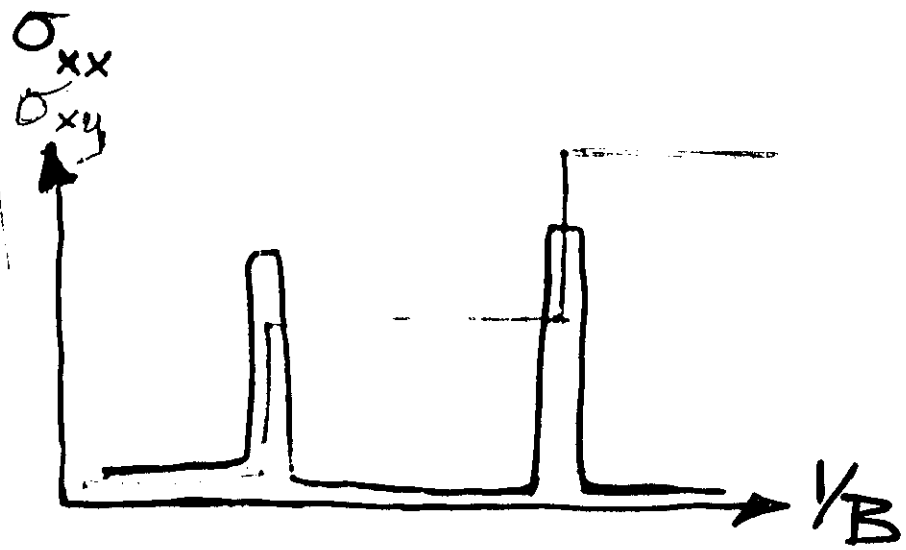

5 Scaling flow diagram

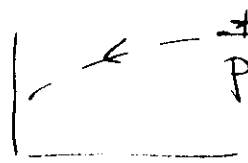

← for increasing B

Flow: how σ varies as length scale at which it is measured increases

implies existence of extended states at only one energy

– and implies picture of σ vs $1/B$.

Linearise flow around delocalisation fixed point

Fixed point at $\sigma_{xx}^*, \sigma_{xy}^*$

$\Delta\sigma_{xy} = \sigma - \sigma^*$

$$\frac{d\,\Delta\sigma_{xy}}{d\ln L} = \frac{1}{\nu}\Delta\sigma_{xy}$$

(ν: exponent!)

$$\frac{d\,\Delta\sigma_{xx}}{d\ln L} = -\phi\,\Delta\sigma_{xx}$$

ϕ: irrelevant

$$\frac{\Delta\sigma_{xy}}{\Delta\sigma_{xy}^0} \sim \left(\frac{L}{L_0}\right)^{1/\nu}$$

$$\xi \sim |\Delta B|^{-\nu}$$

$$\Delta\sigma_{xx} \sim L^{-\phi}$$

(i) $\Delta\sigma_{xy}^0 \propto B - B^*$

(ii) $L \sim \xi \Rightarrow \Delta\sigma_{xy} \sim \mathcal{O}(1)$

So $\xi \sim |\Delta B|^{-\nu}$

(ξ: localisation length)

Dynamic scaling

Correlation time, $\tau \sim \xi^{z} \sim |\Delta B|^{-\nu z} \Rightarrow |\Delta B| \sim T^{1/\nu z}$

z: Dynamic scaling exponent
– interactions hidden here — could influence ν, too

Transparency (6)

Thermal scaling $\frac{1}{\nu z} = 0.42$

Sample size $\nu = 2.3 \Rightarrow z \simeq 1.0$

Transparency (7)

Frequency $|\Delta B| \sim \omega^{1/\nu z}$

Current Finite $\mathcal{E}$-field important when:
field energy ~ Correlation energy

$e\mathcal{E}\xi \sim |\Delta B|^{\nu z}$

$I |\Delta B|^{-\nu} \sim |\Delta B|^{\nu z}$

$|\Delta B| \sim I^{1/\nu(z+1)}$

Expt: $\frac{1}{\nu(z+1)} = 0.21$

Re-entrant insulating phase (Khmelnitskii 84)

Relaxation-time approximation

$\sigma_{xx} = \frac{ne\tau}{m} \frac{1}{1+(\omega_c\tau)^2}$

$\sigma_{xy} = \frac{ne^2\tau}{m} \frac{\omega_c\tau}{1+(\omega_c\tau)^2}$

$\omega_c = \frac{eB}{m}$

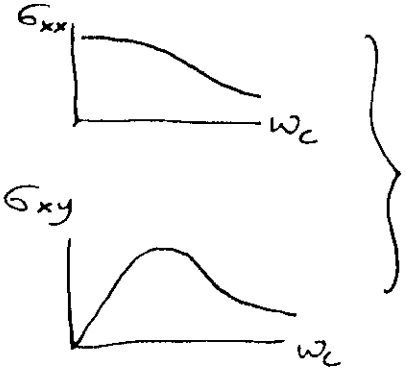

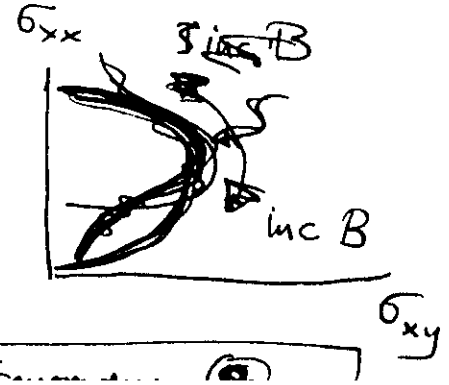

Transparency (8)

Scaling at the Mobility Edge

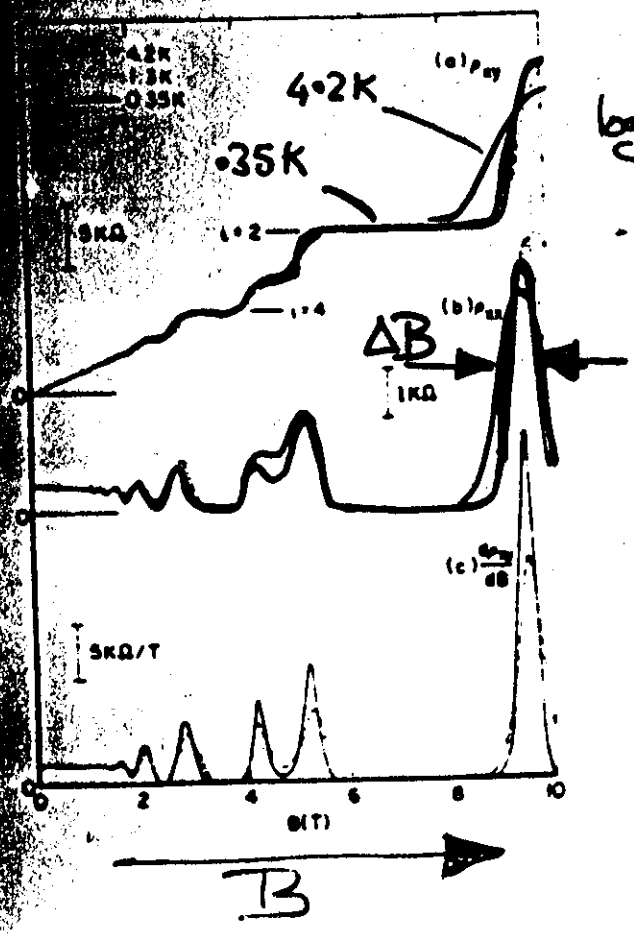

Tsui et al

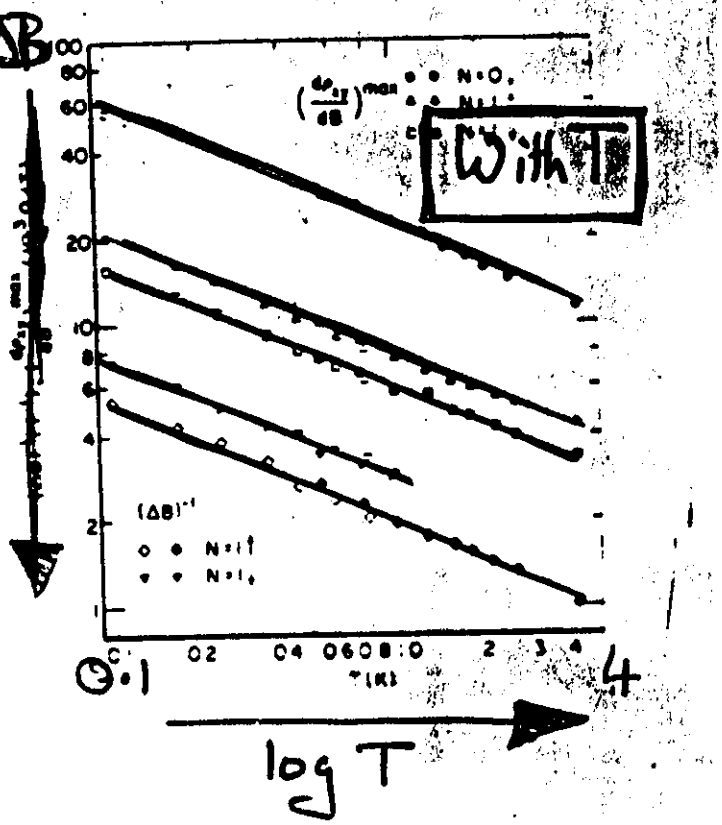

log (ΔB)

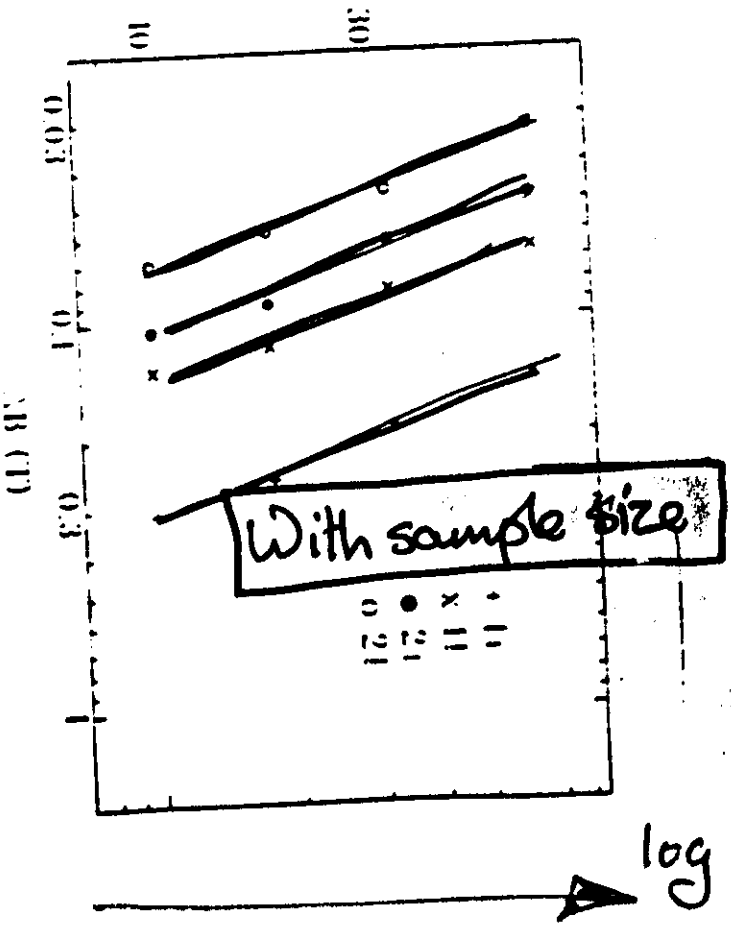

Koch et al

Scaling at mobility edge

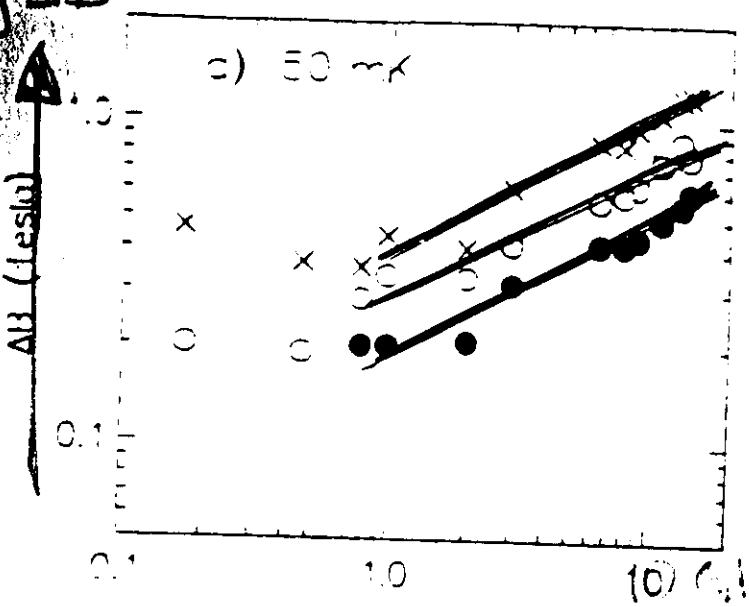

Scaling with frequency

Tsui et al

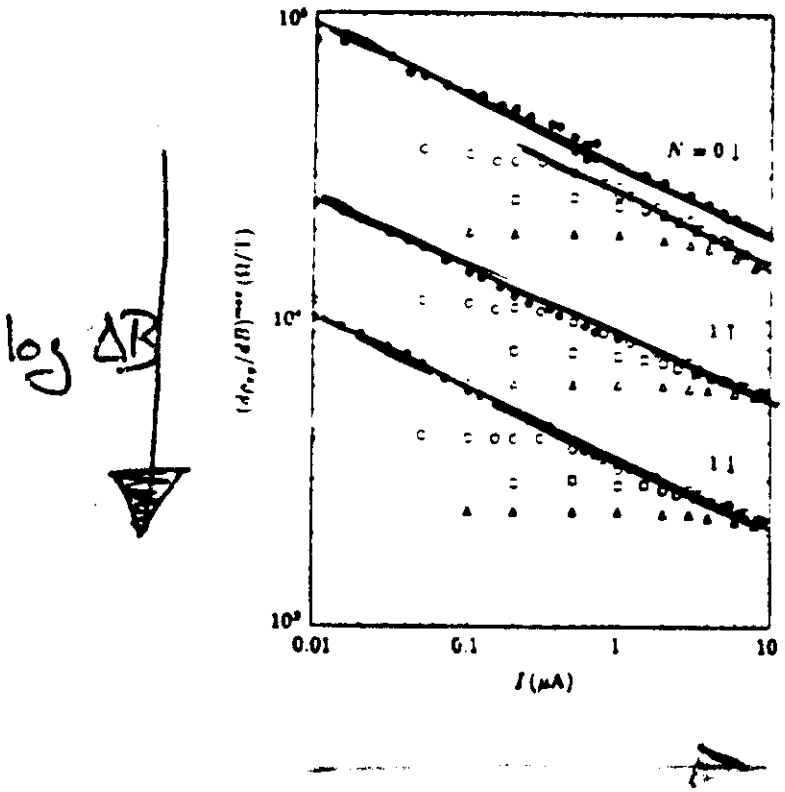

Scaling with Current

Wei et al

Hughes, Pepper et al

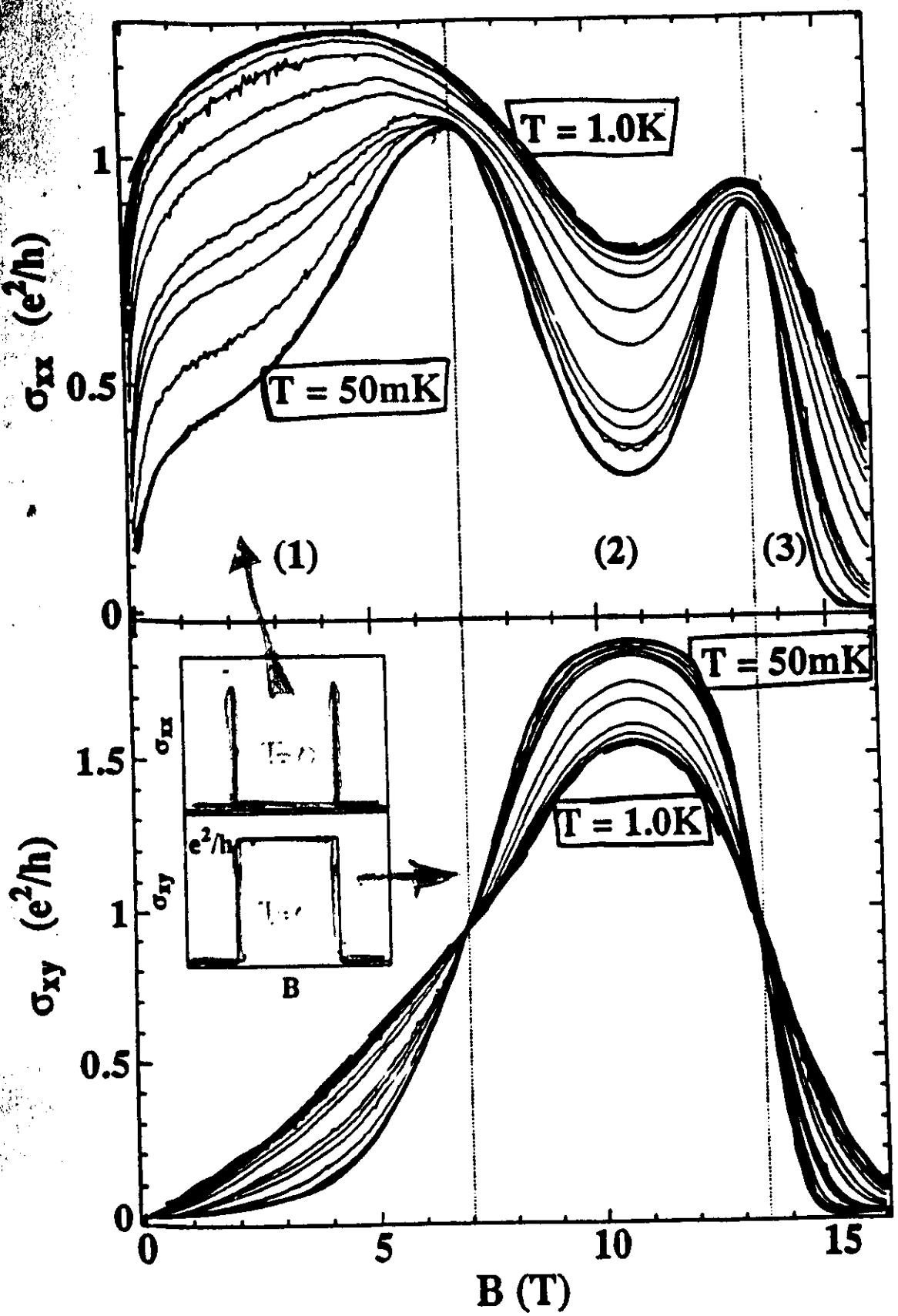

Lectures 2 & 3

Models

Tight-binding
Projection onto one Landau level
Semiclassical (network model)

Numerical Techniques

Diagonalisation
Transfer matrix + finite size scaling
Green function

Results

Exponents
Hall plateau conductance

Objective:

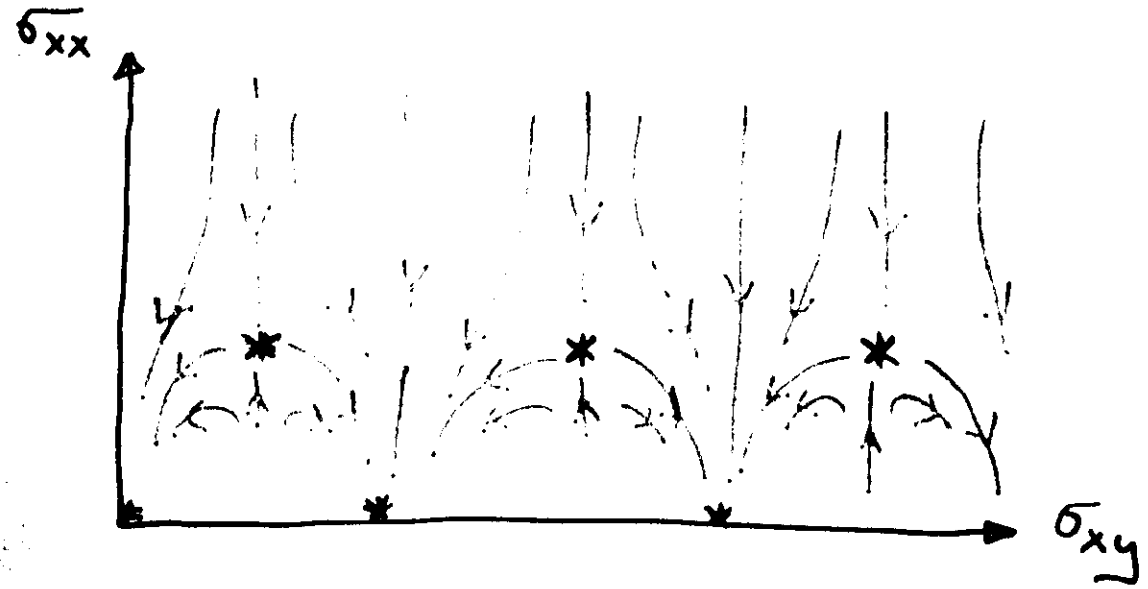

Positions of unstable fixed points (*) ?

How away from fixed points ?

LECTURE 2

Start with scaling flow

Models

with short distance properties

Start: want model which lies at fixed point

Full Theory $H_F = \frac{1}{2m}(\vec{p} - e\vec{A})^2 + V(\underline{r})$

Tight binding model

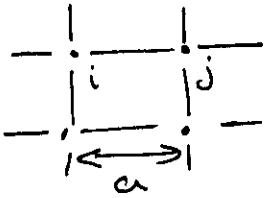

B - field

$t_{ij} \to t_{ij}\, e^{i\frac{e}{\hbar}\int_{r_i}^{r_j} \underline{A}(\underline{r})\cdot d\underline{r}}$

$$H_{TB} = \sum_{ij} t_{ij}\, c_i^\dagger c_j + \sum_i \varepsilon_i c_i^\dagger c_i$$

(ε_i: random)

But want $a \ll \ell_c \ll$ system size

Projection onto one Landau level $(\ell_c = 1)$

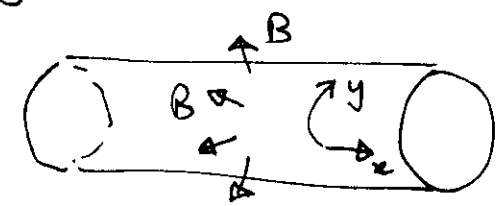

$y + L \equiv y$

$\underline{A} = B(0, Bx, 0)$

$$\langle \underline{r} | n,k \rangle = \frac{1}{\sqrt{L}} e^{iky}\, \varphi_n(x - k)$$

$$P_n \equiv \sum_k |nk\rangle\langle nk|$$

$$H_n = P_n H_F P_n$$

$$= (n+\tfrac{1}{2})\hbar\omega_c + \sum_{kq} |nk\rangle\, U_{kq}\, \langle nq|$$

$$U_{kq} = \langle nk | V(\underline{r}) | nq \rangle$$

Fine for $\lambda \gtrsim \ell_c$

NOT for $\ell_c \ll \lambda$

Network model (semi classical limit)

Show (4) : classical limit

Think in more detail about motion in smooth potential

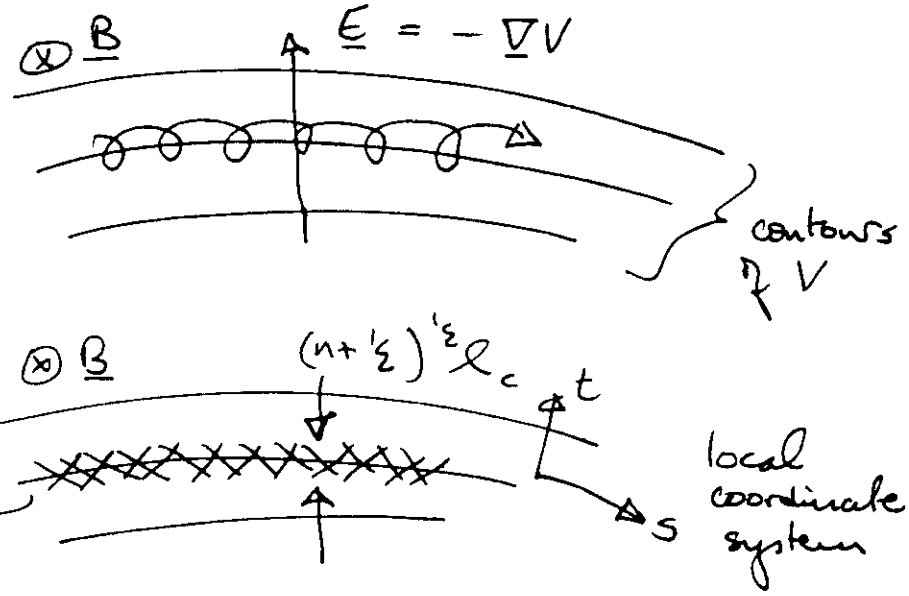

Classical motion
- guiding centre drift

Quantum state

Specify phase + amplitude

Don't care about t-dependence of ψ
Don't care about amplitude & drift velocity separately

Define $z(s)$ by:

(i) $\arg[z(s)] = \arg[\psi(s, t=0)]$

(ii) $|z(s)|^2 = \int dt\ \psi^*(s,t)\ \hat{J}_s\ \psi(s,t)$

(a) Consider long piece of contour

$z(s_2) = e^{i\phi} z(s_1)$

[Fixed ϕ for all. $z \in \mathbb{C}$]

(b) Tunnelling at saddle points

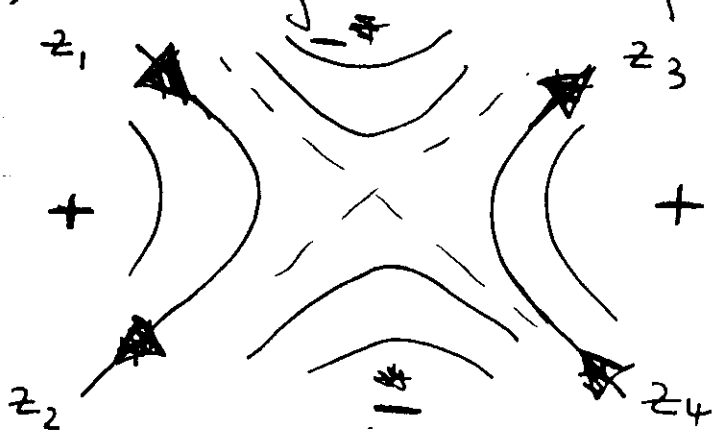

(i) Linearity of Schrödinger eqn implies

$$\begin{pmatrix} z_3 \\ z_4 \end{pmatrix} = \underset{\sim}{M} \begin{pmatrix} z_1 \\ z_2 \end{pmatrix} \quad \text{or} \quad \underline{R} = \underset{\sim}{M}\,\underline{L}$$

(ii) Current conservation

Net current (left → right) is

$$|z_1|^2 - |z_2|^2 \equiv \underline{L}^+ \sigma_z \underline{L} = \underline{R}^+ \sigma_z \underline{R}$$

$$= \underline{L}^+ (\underset{\sim}{M}^+ \sigma_z \underset{\sim}{M}) \underline{L} \qquad \text{for all } \underline{L}$$

$$\Rightarrow \quad \sigma_z = \underset{\sim}{M}^+ \sigma_z \underset{\sim}{M}$$

General solution (simple but tedious algebra!)

$$\underset{\sim}{M} = \begin{pmatrix} e^{i\alpha} & \\ & e^{i\beta} \end{pmatrix} \begin{pmatrix} \cosh\theta & \sinh\theta \\ \sinh\theta & \cosh\theta \end{pmatrix} \begin{pmatrix} e^{i\gamma} & \\ & e^{i\delta} \end{pmatrix}$$

$\alpha, \beta, \gamma, \delta$ & θ real

Alternatively, could relate top & bottom amplitudes instead of left + right

ie. $\begin{pmatrix} z_2 \\ z_4 \end{pmatrix} = \tilde{M} \begin{pmatrix} z_1 \\ z_3 \end{pmatrix}$

same form for $\tilde{M}$, with $\sinh\tilde{\Theta} = 1/\sinh\Theta$

Significance of Θ ?

(a) $\Theta \to 0 \Rightarrow z_3 = z_1$, $z_4 = z_2$

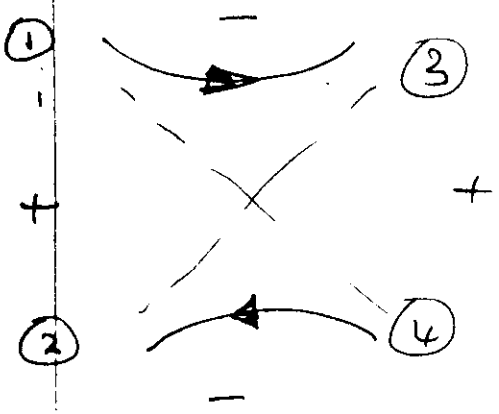

low energy limit

(b) $\Theta \to \infty \Rightarrow z_2 = z_1$, $z_4 = z_3$

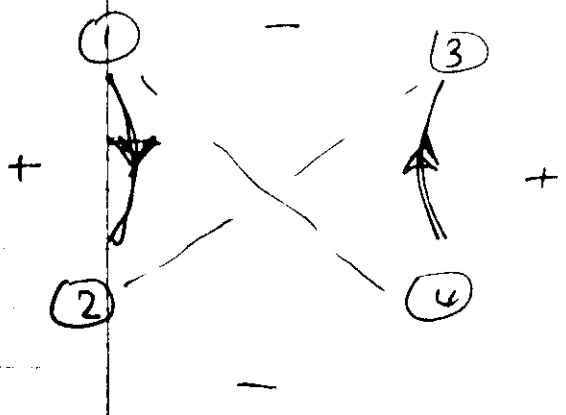

high energy limit

Show (5)

simplest case: ϕ uniformly distributed topology, Θ non-random

Network model for spin-split Landau level

Correlation length of disordered potential $\gg$ magnetic length

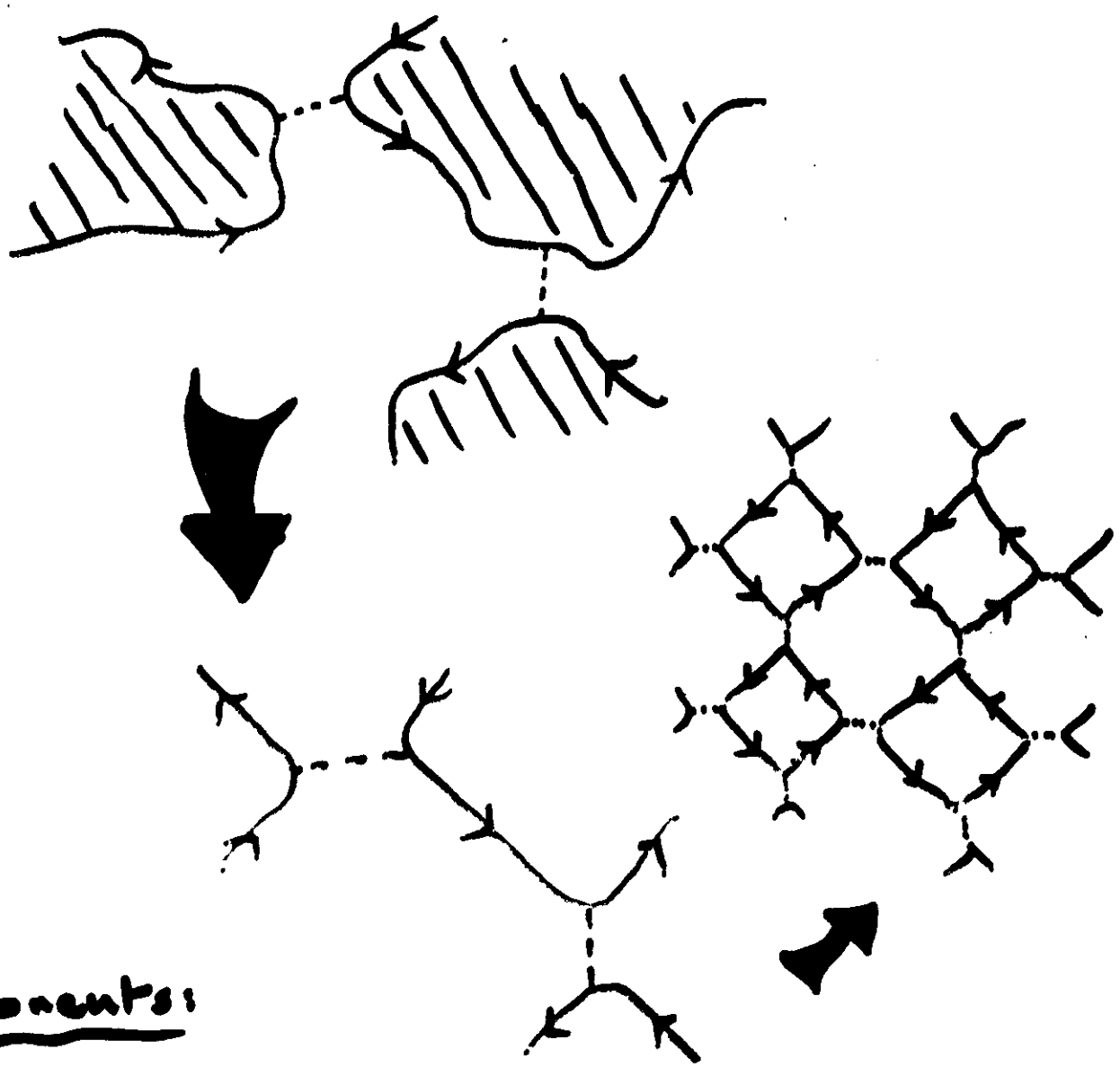

Components:

link

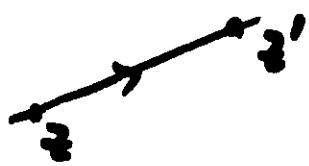

$$z' = e^{i\phi} z$$

node

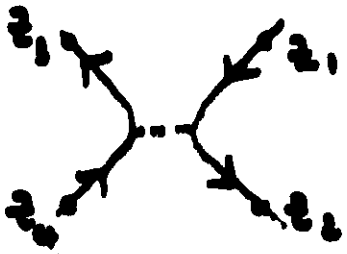

$$\begin{pmatrix} z_3 \\ z_4 \end{pmatrix} = \begin{pmatrix} \cosh\theta & \sinh\theta \\ \sinh\theta & \cosh\theta \end{pmatrix} \begin{pmatrix} z_1 \\ z_2 \end{pmatrix}$$

Methods

Return to projection onto one Landau level

Diagonalisation

Limitations: storage $N \times N$ matrix $N = 10^3 \Rightarrow 8$ Mb
$N = L^2 \Rightarrow$ storage $\sim L^4$ Mention Lanczos

2d: Weak localisation ξ exponentially large
hard to distinguish $\xi \gg$ system size from $\xi = \infty$

Show ① : Huo & Bhatt

① : Identify extended states from sensitivity to boundary conditions
ΔE & N_{ext} vs $N \rightarrow \nu$

Show scaling flow diagram

Investigate $\sigma_{xy}^* = n + \frac{1}{2}$

Show Huo, Helzel & Bhatt

Scaling on strips

Benettin et al 1980
Pichard & Sarma 1981
MacKinnon & Kramer 1981

Limitation : time
System : $M \times \infty$
Storage $\sim M$

Big advance
Study quasi-one D → states always localised
→ $\xi(M)$ vs M
→ scaling analysis of data

Skolt Study scattering properties of long sample

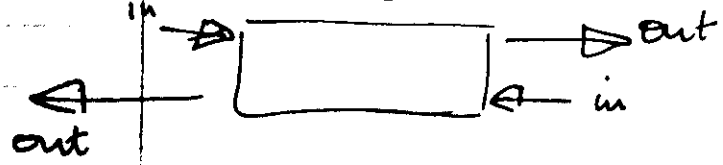

$|out\rangle = S|in\rangle$

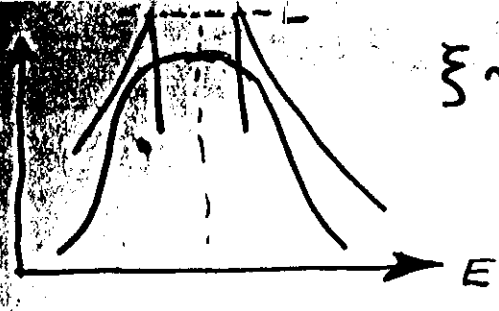

$\xi \sim |\Delta E|^{-\nu}$ $\quad \xi = L \rightarrow \Delta E \sim L^{-1/\nu}$

$$\Delta E \sim N^{-1/2\nu}$$

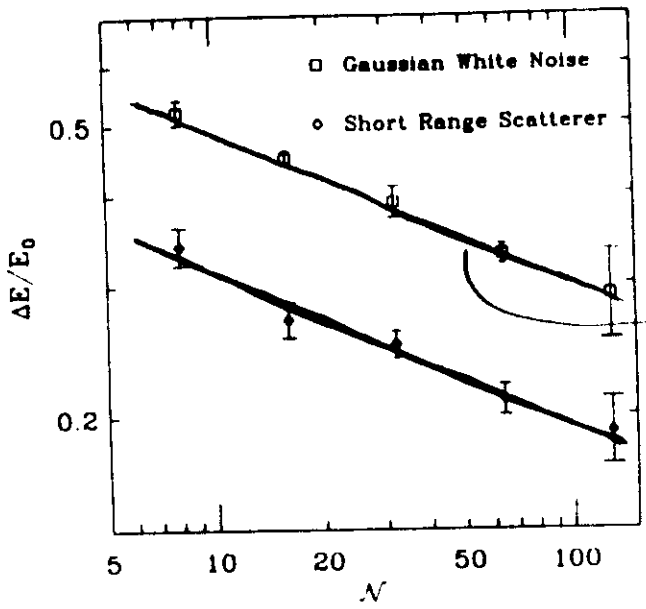

$\log \Delta E$ ↑ $\qquad \frac{1}{2\nu} = 0.21$

$\log N$ →

Hwa & Bhatt '92

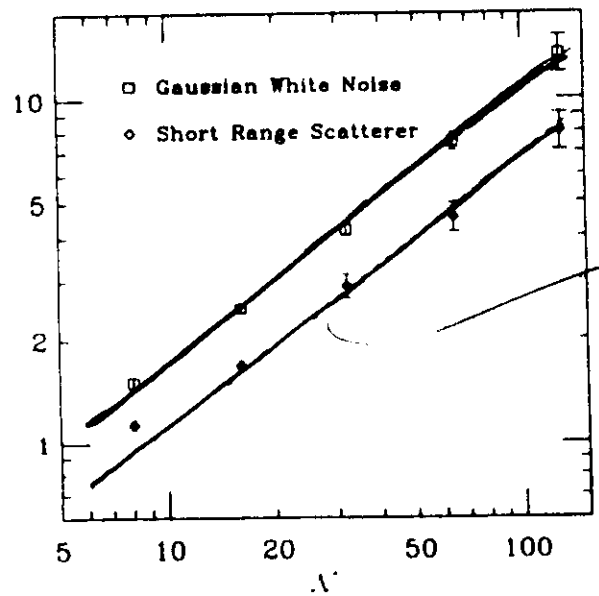

$\log N_{ext}$ ↑ $\qquad 1 - \frac{1}{2\nu} = 0.79$

$\log N$ →

$\nu = 2.3$

$N_{ext} \sim N \Delta E$

$$N_{ext} \sim N^{1 - 1/2\nu}$$

Asymmetric potential distribution

$$P[V(x)] \neq P[-V(x)]$$

$\rho(E)$

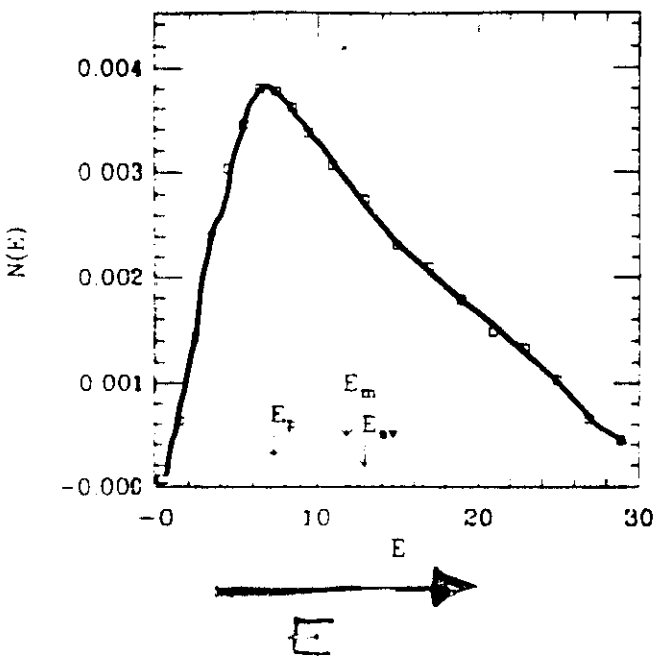

E

Huo, Hetzel & Bhatt '93

N=16

σ_{xy}

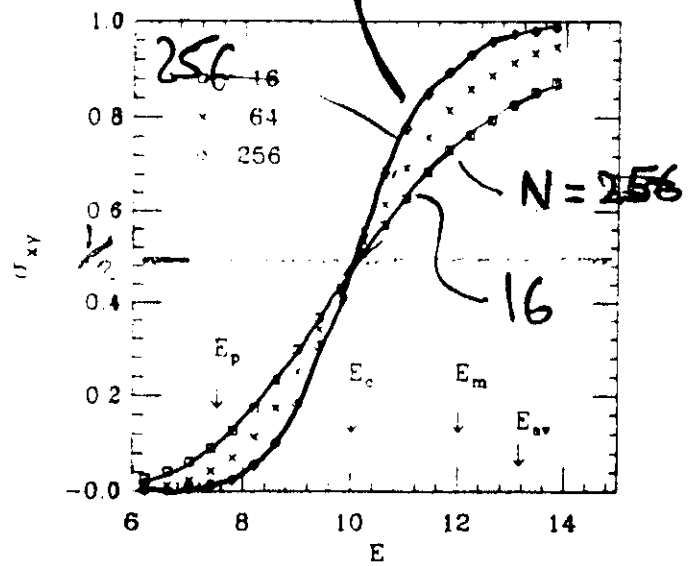

L

But want to construct sample iteratively

- use transfer matrix instead of S-matrix

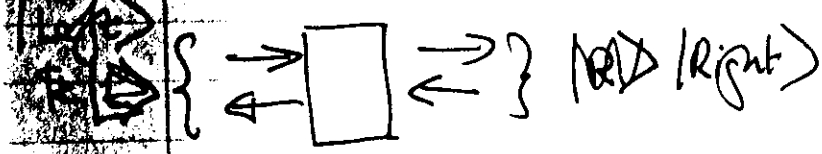

$|Right\rangle |R\rangle = M |R\rangle |Left\rangle$

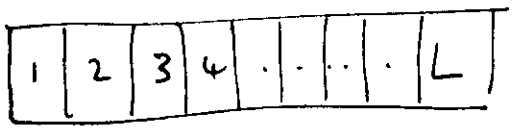

$|Right\rangle = T_L |Left\rangle$

$T_L = M_L M_{L-1} \cdots M_2 M_1$

Problem to understand limiting behaviour of product of many random matrices

c.f. Central limit theorem

$S_L = \sum_{i=1}^{L} x_i \Rightarrow \langle S_L \rangle = L \langle x \rangle \quad , \quad \Delta S = L^{1/2} \Delta x$

Here (i) multiplication not addition
(ii) don't commute

(i) Only $P_L = \prod_{i=1}^{L} z_i$

$\arg(P_L) \sim$ uniform

$\log |P_L| \sim L \langle |\log z| \rangle$

$|P_L| \sim e^{L/\xi}$ but log-normally distributed

~~Here~~ $\xi^{-1} = \langle |\log z| \rangle$

Oseledec's theorem

$$(T_L^+ T_L)^{\frac{1}{2L}} = U^+ D U$$

(D: diagonal; U: unitary)

As $L \to \infty$

D : limiting value
U : limiting distribution

Current conservation

$$T = \begin{pmatrix} u & 0 \\ 0 & v \end{pmatrix} \begin{pmatrix} \cosh\theta & \sinh\theta \\ \sinh\theta & \cosh\theta \end{pmatrix} \begin{pmatrix} u' & 0 \\ 0 & v' \end{pmatrix}$$

($2M \times 2M$; $M \times M$ blocks)

LECTURE 3

θ : diagonal matrix

Eigenvalue k is $e^{\theta_{kk}} \sim e^{L/\xi_k}$

& eigenvalue $2M+1-k$ is $e^{-\theta_{kk}}$

$1/\xi$'s : Lyapunov exponents

Physical quantities?

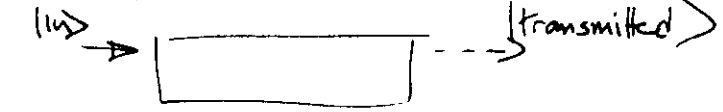

$|\text{transmitted}\rangle = t\,|\text{in}\rangle$

($M \times M$ transmission matrix)

$$t = u \frac{1}{\cosh\theta} u'$$

$$t_{MM} \sim e^{-L/\xi_{max}}$$

We need $\xi_{max}(M)$

As function of model parameters & of M

Numerical method

Non-random problem

NN matrix H $\quad H\underline{u}_i = \lambda_i \underline{u}_i$

$\lambda_1 > \lambda_2 > \cdots \lambda_N$ $\quad \{\underline{u}_i$ complete$\}$

$\underline{x}$: arbitrary initial vector

Consider $(H)^L \underline{x}$

with $\underline{x}_1 = \sum_i a_i \underline{u}_i$

$$(H)^L \underline{x}_1 = \sum_i \lambda_i^L a_i \underline{u}_i = \lambda_1^L \sum_i a_i \left(\frac{\lambda_i}{\lambda_1}\right)^L \underline{u}_i$$

$$\sim \lambda_1^L a_1 \underline{u}_1 \quad \text{as } L \to \infty$$

$$\text{So } \frac{1}{L} \log \left|(H)^L \underline{x}\right| = \log(\lambda_1) + \Theta(1/L)$$

To get λ_2

Consider $\underline{x}_1, \underline{y}_1 = \sum_i b_i \underline{u}_i$

$$\underline{y}_L - \frac{(\underline{x}_L^T \cdot \underline{y}_L)\,\underline{x}_L}{|\underline{x}_L|^2} \sim b_2 \lambda_2^L \underline{u}_2$$

like wise for $\lambda_3, \lambda_4 \cdots$

1-d Example

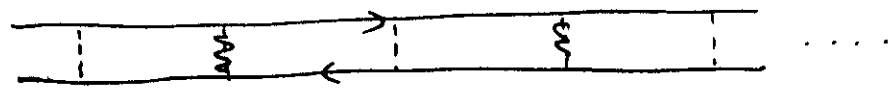

$$\begin{pmatrix} c & s \\ s & c \end{pmatrix}\begin{pmatrix} e^{i\phi} & \\ & e^{i\phi'} \end{pmatrix} \quad \begin{pmatrix} c & s \\ s & c \end{pmatrix} \begin{pmatrix} e^{i\phi''} & \\ & e^{i\phi'''} \end{pmatrix} \begin{pmatrix} c & s \\ s & c \end{pmatrix}$$

Eigenvectors: Consider $\underline{x}$

Eigenvectors of $\begin{pmatrix} c & s \\ s & c \end{pmatrix}$ are $\frac{1}{\sqrt{2}}\begin{pmatrix} 1 \\ \pm 1 \end{pmatrix}$ eigenvalues $e^{\pm\theta}$

$$\underline{x}_1 = \cos\phi\, \underline{u}_1 \; e^{i\alpha}\cos\phi\, \underline{u}_1 + e^{i\beta}\sin\phi\, \underline{u}_2$$

$$\frac{1}{\xi} = \frac{1}{L}\log|\underline{x}_L| = \frac{1}{2\pi}\int_0^{2\pi} d\phi \log\left[e^{2\theta}\cos^2\phi + e^{-2\theta}\sin^2\phi\right]^{1/2}$$

$$= \log(\cosh\theta)$$

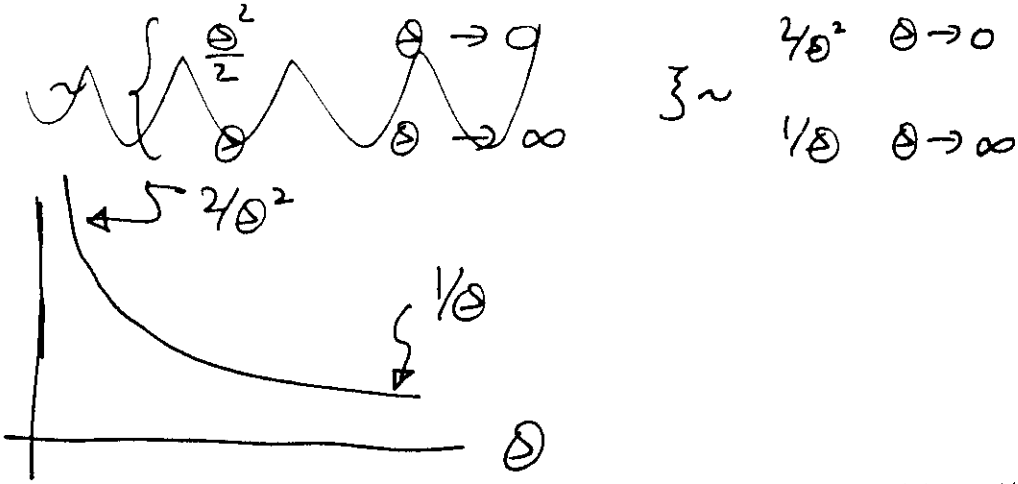

States always localised in 1-D

Quasi one dimensional system

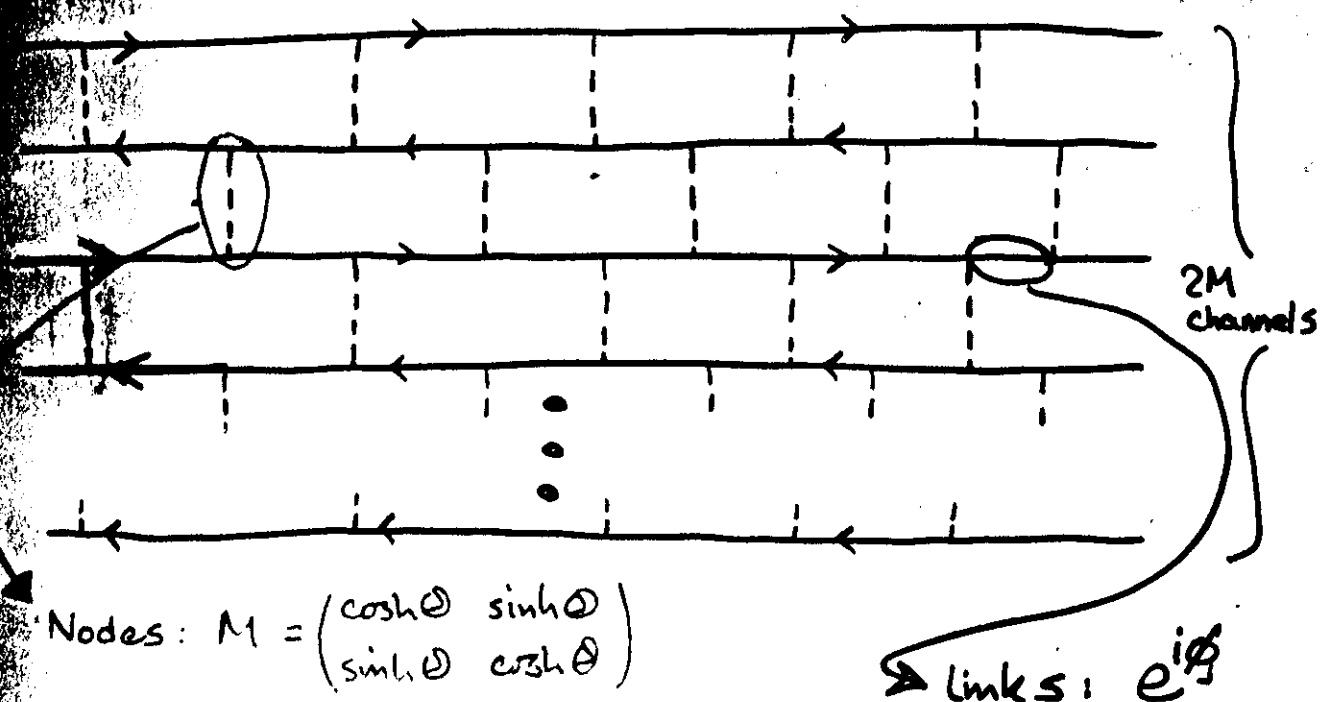

Calculate localisation length $\xi_M(\Theta)$

As function of:

$\Theta \approx$ energy in Landau level

$M \equiv$ system width

Numerical results

Show ③, ③a, ③b Network model
– localised states as $\theta \to 0$ & $\theta \to \infty$

What to expect?

Localised states

$$\lim_{M\to\infty} \xi_M(\theta) = \xi_{Bulk}(\theta)$$

Extended states

$\xi_M(\theta)$ increases with M

[In fact $\xi_M \propto M^{d-1}$]

So $\frac{\xi_M(\theta)}{M} \to \begin{cases} 0 & \text{localised} \\ \text{constant} > 0 & \text{critical point} \end{cases}$

Show ④ ξ_M/M

~~Data Analysis~~ One parameter scaling analysis

How to get most from data?

Simplest approach: $\xi_{Bulk} = \lim_{M\to\infty} \xi_M$

very hard to reach limit except in band tails

Instead

$$\xi_M(\theta) = M\, f\left(\xi_{Bulk}(\theta)/M\right)$$

↑ function of one variable only

Scaling analysis – continued

Re write as

$$\log\left(\frac{\Xi_M(\theta)}{M}\right) = g\left[\log\left(\frac{\Xi_{Bulk}(\theta)}{M}\right)\right]$$

Show (5a), (5b) (5c)

Shifts → ~~choices of~~ fits for $\log[\Xi_{Bulk}(\theta)]$

Show (6) → Divergence of $\Xi_{Bulk}(0)$

~~Fixed point~~

Universal fixed point for σ_{xx}^*

Show (4): $\frac{\Xi_M(\theta)}{M}$ vs θ

What does $\lim_{M\to\infty} \frac{\Xi_M(\theta)}{M}\Big|_{\theta=\theta_c} \equiv \alpha^*$ tell us ?

Want to interpret it as σ_{xx}^*

Problem: Ξ_M comes from studying long strips → conductance exponentially small

Had

$$\underset{\sim}{t} = \underset{\sim}{u}\,\frac{1}{\cosh\underset{\sim}{\theta}}\,\underset{\sim}{u}' \qquad [\underset{\sim}{u}, \underset{\sim}{u}', \underset{\sim}{\theta}\ M\times M \text{ matrices}]$$

Landauer: $G = \mathrm{tr}\left[\underset{\sim}{t}\,\underset{\sim}{t}^+\right] = \sum_k \frac{1}{\cosh^2\theta_{kk}}$

θ_{kk} = $\nu_k L$ & $\nu_k = k\cdot\nu_1 = k\,\frac{\alpha^* - \alpha^*}{M\alpha^*}$

So $G = \sum_k \frac{1}{\cosh^2\left(k\frac{\alpha^* L}{M\alpha^*}\right)} = \frac{M}{L}\frac{\alpha^*}{\alpha^*}\int_0^\infty dx\,\frac{1}{\cosh^2(x)}$ So $\sigma_{xx}^* = \text{Const.}\times\frac{L}{\alpha^*}$

Show ⑦ flow to fixed value of $\frac{\Sigma_M}{M}$ ≡ flow to σ_{xx}^*

Approach to fixed point

Show scaling flow diagram

$$\frac{d\,\Delta\sigma_{xx}}{d\ln L} = -\phi\,\Delta\sigma_{xx}$$

$$\Rightarrow \quad \Delta\sigma_{xx} = L^{-\phi}$$

Show ⑧

See also

Huckestein & Kramer

Phys Rev Lett 64 1437 (1990)

Chalker & Coddington '88

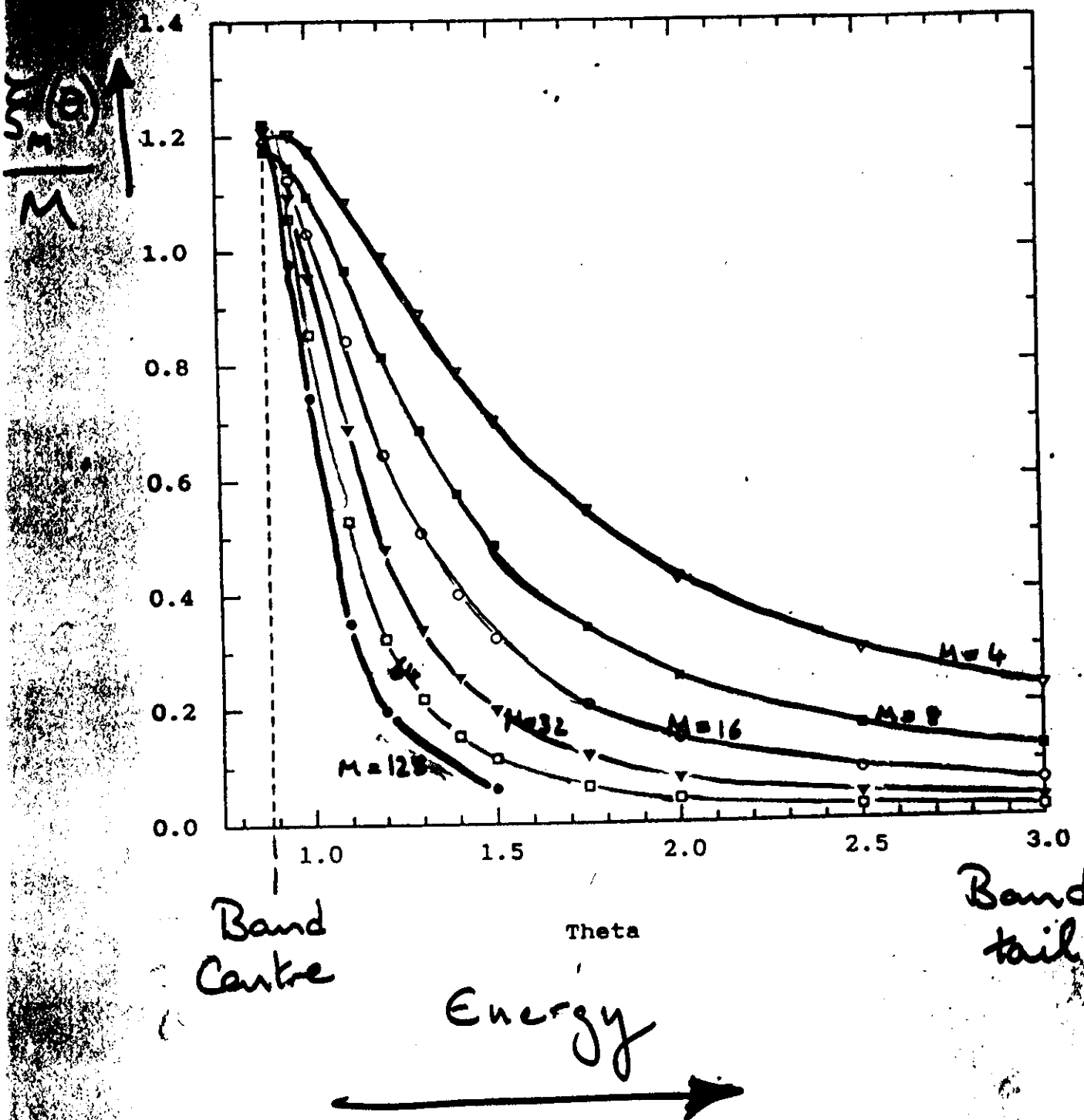

One parameter scaling

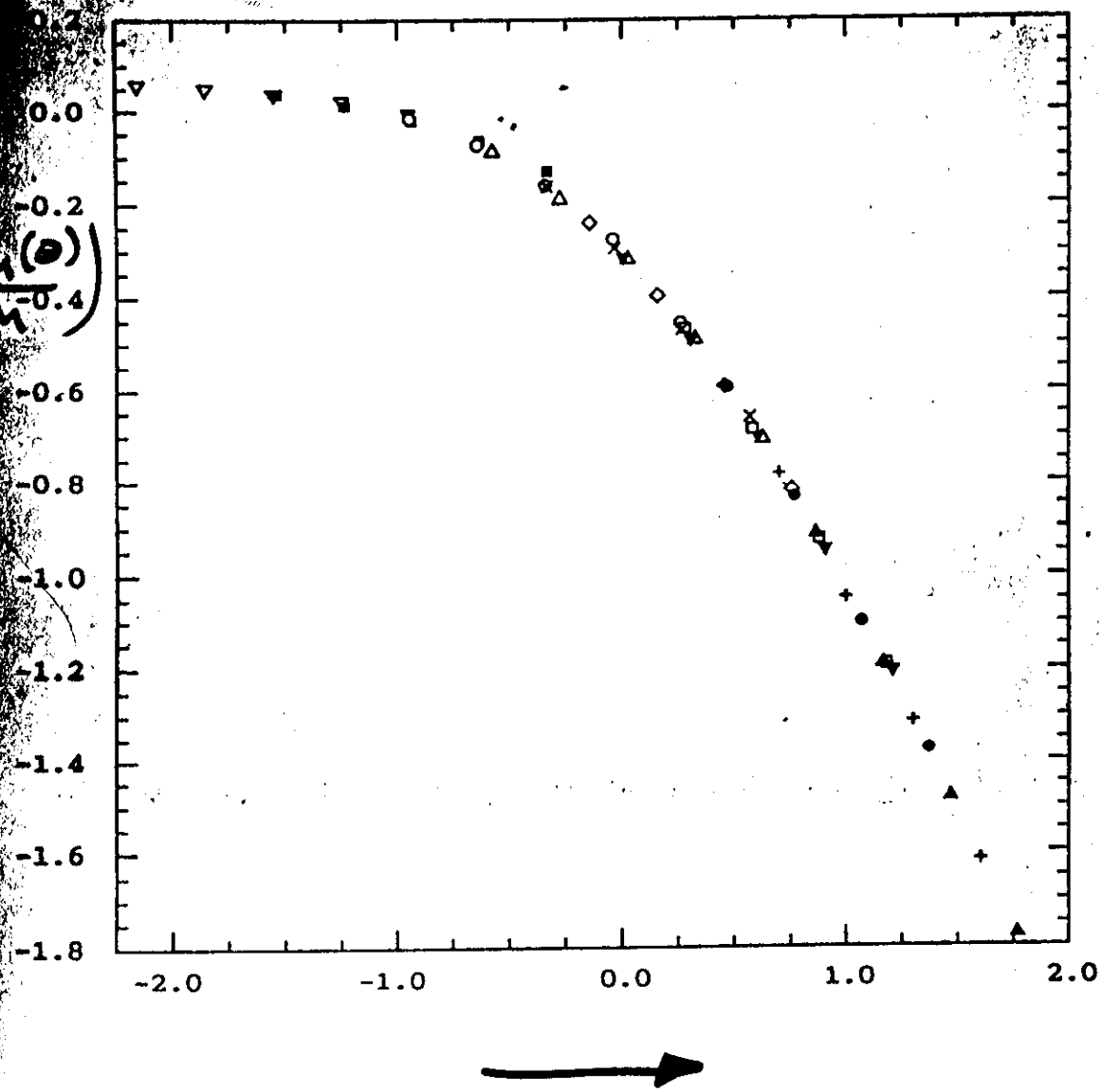

$\frac{\xi_H(\theta)}{M}$

$\log_{10}\left(\xi_\infty(\theta)/M\right)$

Fig 6

$\ln[\xi_{Bulk}(\Theta)]$

Lee, Wang & Kivelson '93

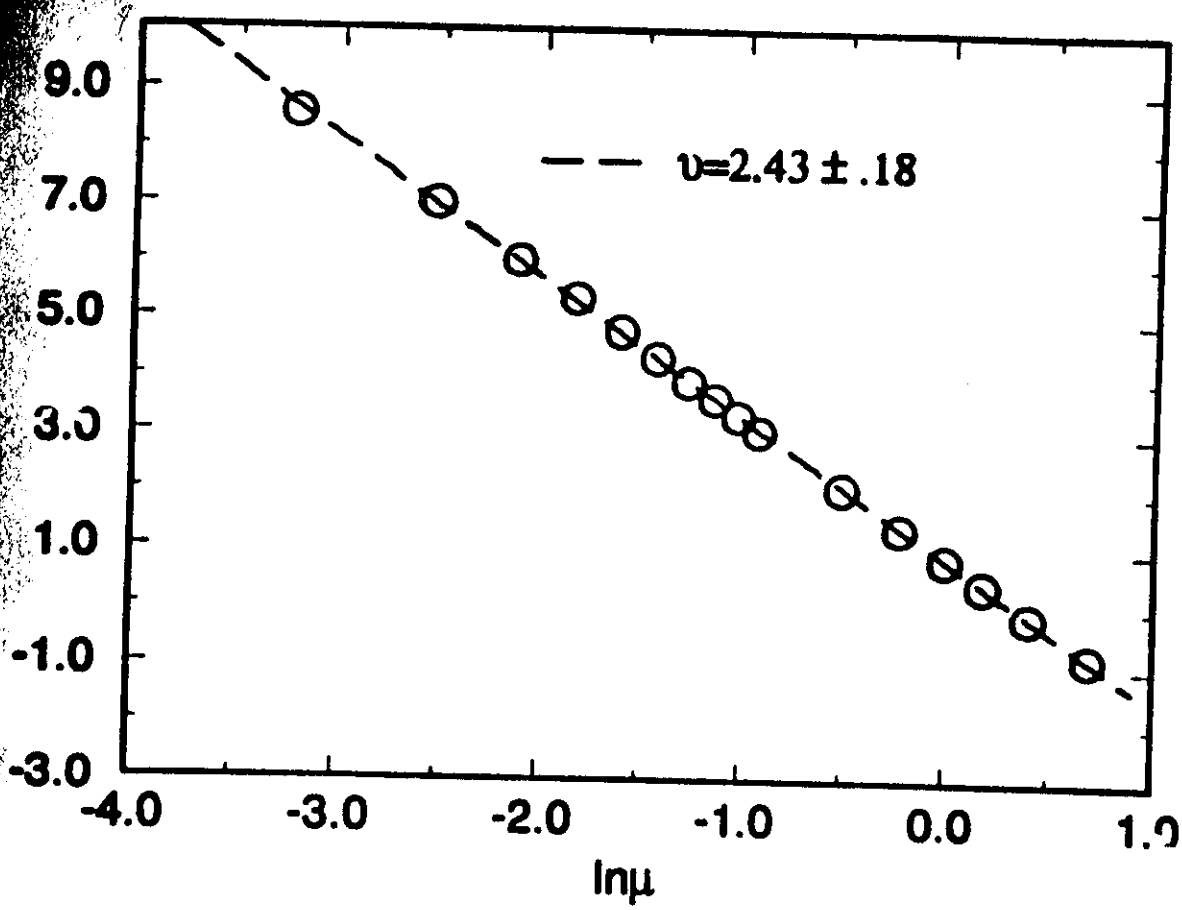

$\ln(\xi)$

$\log|\Theta - \Theta_c|$

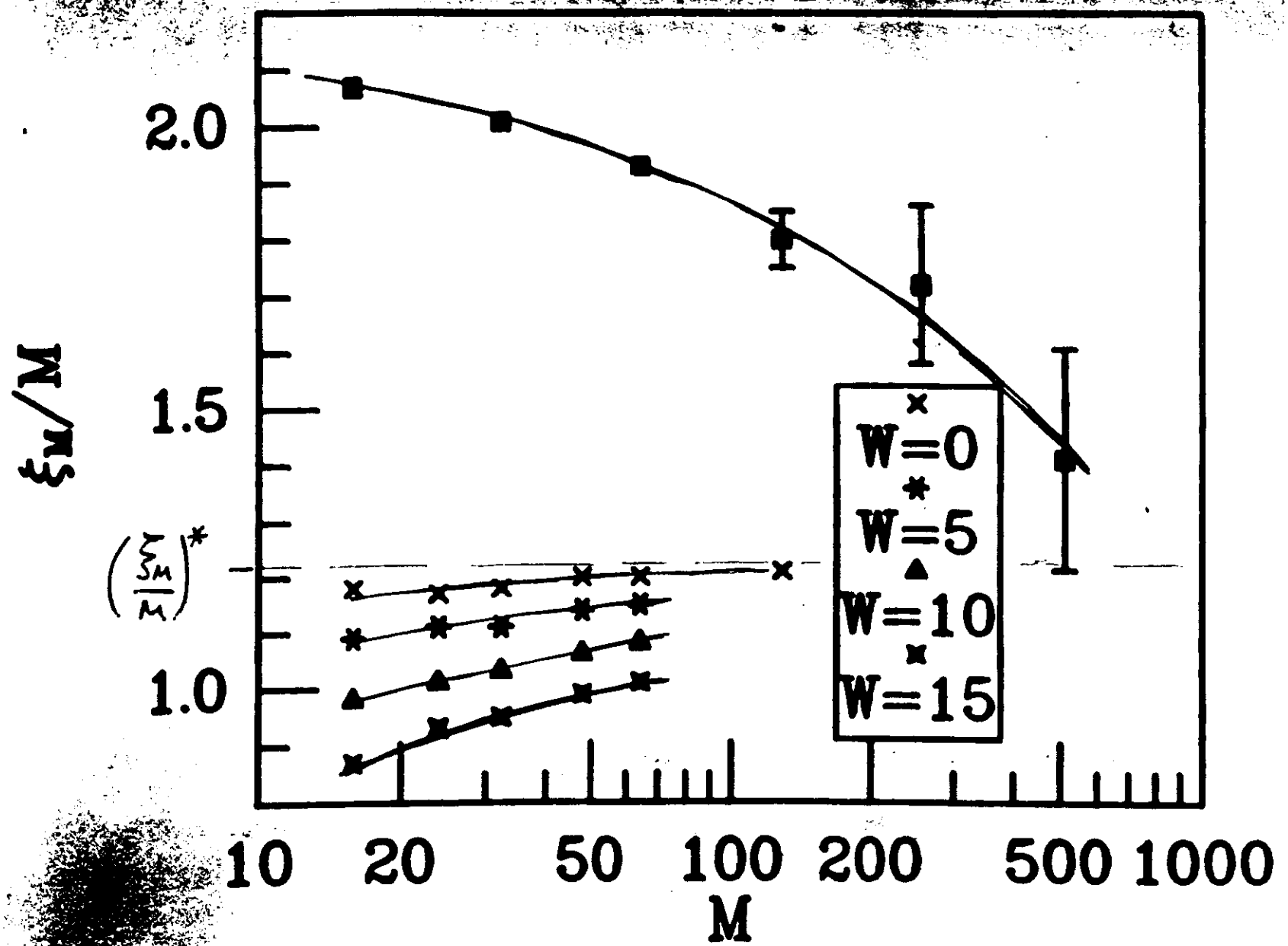
2.0
1.5
1.0
ξ_M/M
$\left(\frac{\xi_M}{M}\right)^*$
W=0
W=5
W=10
W=15
10
20
50
100
200
500
1000
M

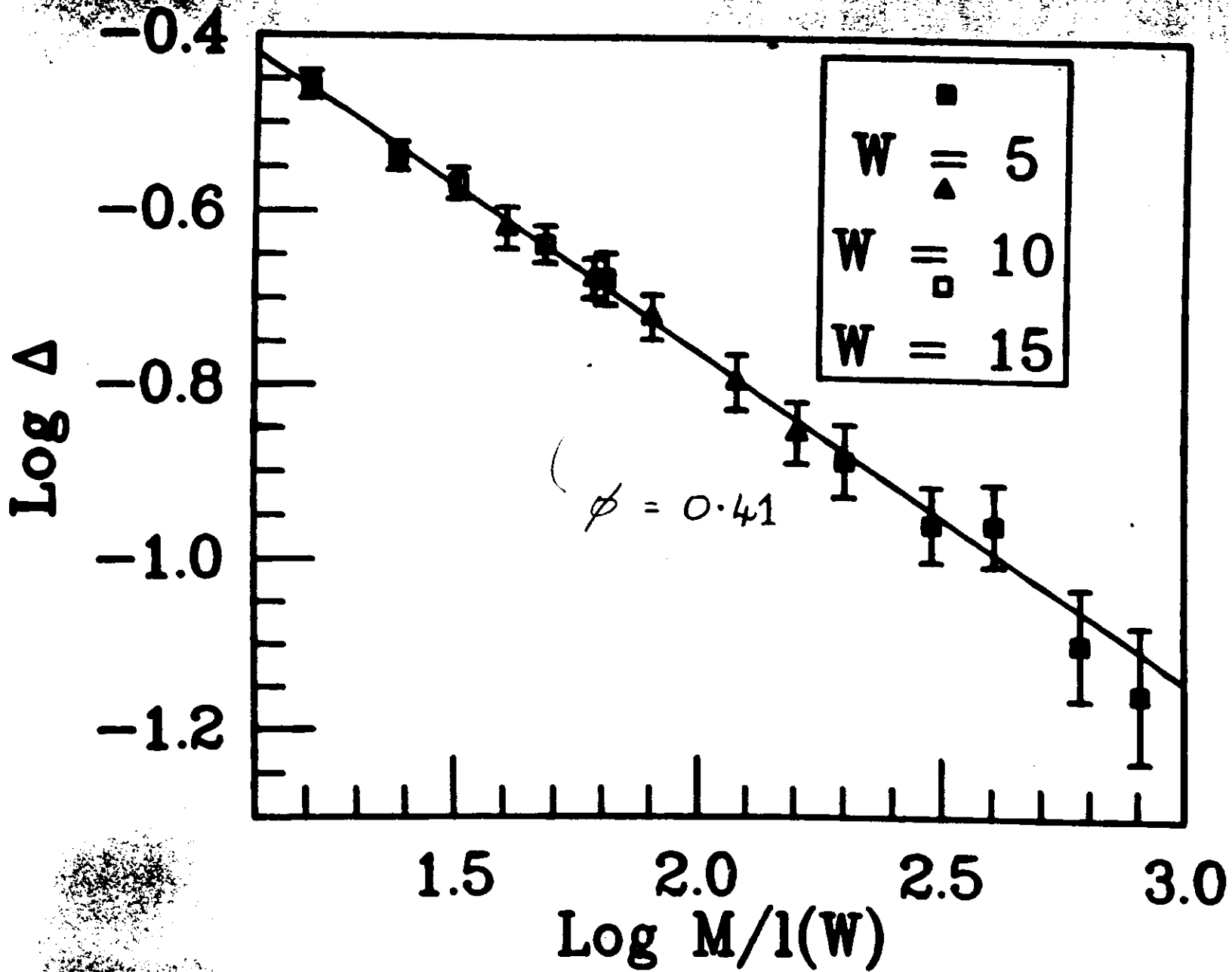
−0.4
−0.6
−0.8
−1.0
−1.2
Log Δ
W = 5
W = 10
W = 15
φ = 0·41
1.5
2.0
2.5
3.0
Log M/l(W)

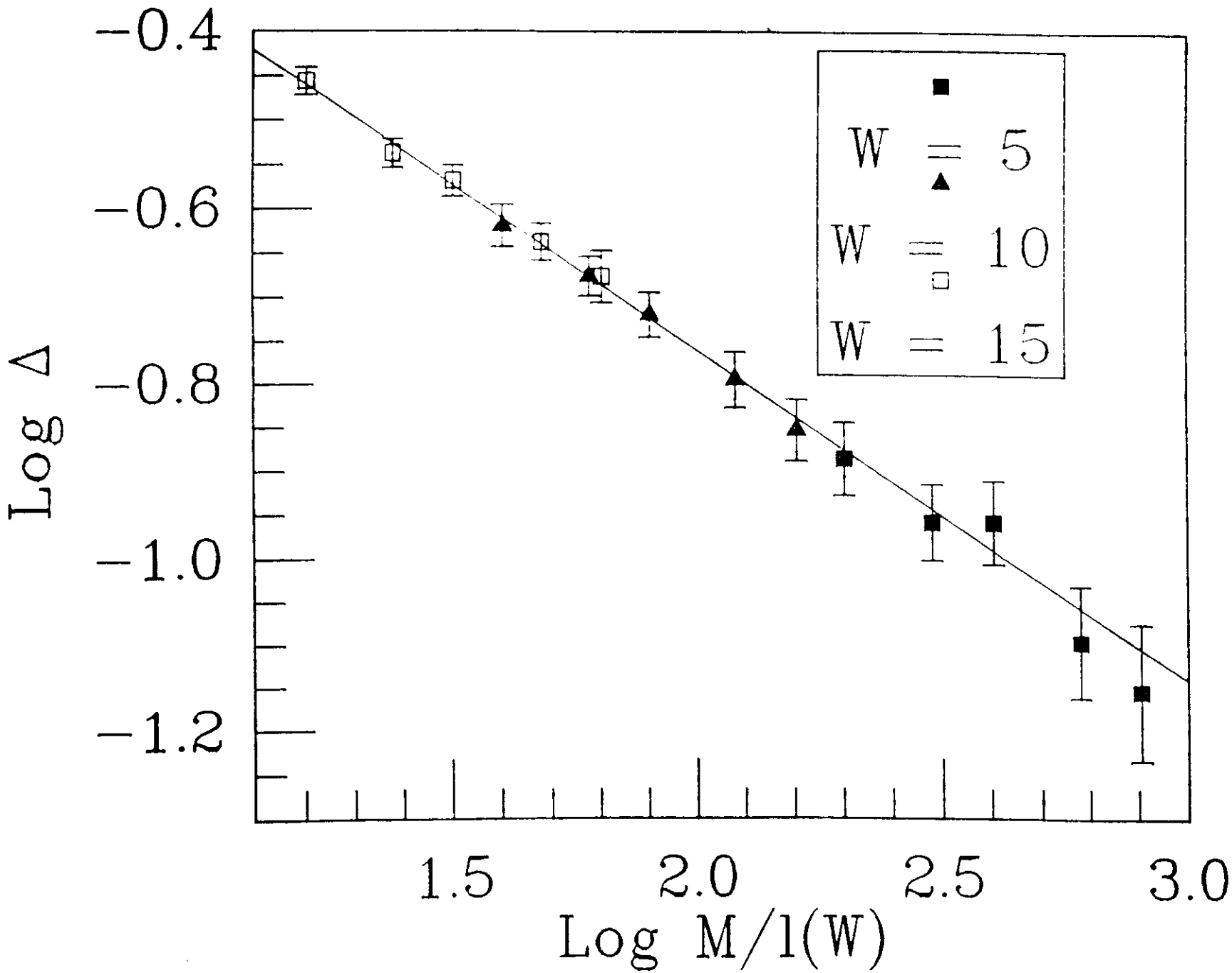
−0.4
−0.6
−0.8
−1.0
−1.2
Log Δ
1.5
2.0
2.5
3.0
Log M/l(W)
W = 5
W = 10
W = 15

LECTURE (4)

Scaling, Diffusion, and the Integer Quantized Hall Effect

J. T. Chalker and G. J. Daniell
Physics Department, Southampton University, Southampton SO9 5NH, United Kingdom
(Received 4 April 1988)

The behavior of the two-particle spectral function, $S(q,\omega)$, is examined in the hydrodynamic regime, at the mobility edge in a model for the integer quantized Hall effect. Results are presented from numerical diagonalization of the Hamiltonian for finite systems. For q^2/ω small, $S(q,\omega)$ has a conventional, diffusive form. For q^2/ω large, the novel dependence $S(q,\omega)\sim\omega^{-\eta/2}q^{-2+\eta}$ is obtained, with $\eta=0.38\pm0.04$.

PACS numbers: 71.50.+t, 71.55.Jv, 72.20.My

Scaling behavior near a mobility edge—viewed as a critical point—is widely believed to be especially simple, at least in the absence of magnetic effects and interactions.[1] This simplicity is a consequence of the one-parameter scaling assumption,[1] that a length-dependent dimensionless conductance is the only quantity necessary to characterize behavior at a given length scale. As a result there is only one independent critical exponent say the localization-length exponent ν, which describes the approach to the mobility edge and from which other exponents, for example, the one for conductivity, can be determined. Correspondingly, at the mobility edge itself, the requirement of homogeneity under combined length and energy scale transformations determines the scaling form of eigenfunction correlations completely.[1] One implication is that the exponent η, governing correlations at the mobility edge, should be given exactly in d dimensions by $\eta=2-d$.

Observation of the integer quantized Hall effect indicates a breakdown of one-parameter scaling. Pruisken and co-workers[2] have shown how this happens within an effective field theory: The Hall conductance appears as a second coupling constant, in addition to the dissipative conductance, and two-parameter scaling emerges.

We describe in this Letter a distinct and striking aspect of the failure of one-parameter scaling at the mobility edge in a model for the integer quantum Hall effect. Eigenfunction correlations do not have a conventional, diffusive form: Although homogeneous, they are characterized by a nontrivial value of η. Equivalently, the diffusion constant (proportional to the dissipative conductance) has a novel wave-vector and frequency dependence: Eq. (2).

Our main results are from numerical diagonalization of the model Hamiltonian. Before describing these calculations, we introduce the quantity studied, the two-particle spectral function, and summarize scaling arguments, our conclusions, and previous analytical work.

The two-particle spectral function is defined by

$$S(\mathbf{r};E,\omega)=\left\langle\sum_{\alpha,\beta}\delta(E-\omega/2-E_\alpha)\delta(E+\omega/2-E_\beta)\psi_\alpha(\mathbf{0})\psi_\alpha^*(\mathbf{r})\psi_\beta(\mathbf{r})\psi_\beta^*(\mathbf{0})\right\rangle,$$

where $\psi_\alpha(\mathbf{r})$ and $\psi_\beta(\mathbf{r})$ are eigenfunctions with energies E_α and E_β and the angular bracket $\langle\rangle$ denote an average over an ensemble of disordered systems. It, or its Fourier transform $S(q;E,\omega)$, determines the system's linear response to time- and space-dependent variations of the chemical potential. The connection between the spectral function and the retarded-advanced two-particle Green's function, and a Ward identity[3] for the latter, restrict the form for small q,ω to be

$$S(q;E,\omega)=\rho(E)h(q,\omega)/\pi[\omega^2+h^2(q,\omega)]$$

with $h(q=0,\omega)=0$, where $\rho(E)$ is the density of states in energy, per unit d-dimensional volume.

If a wave packet, constructed as a superposition of eigenstates close in energy to E, spreads diffusively for long times and for large distances with diffusion constant D, then $h(q,\omega)=\hbar Dq^2$ for small q,ω. More generally, if $E=E_c$, the mobility edge energy, then $h(q,\omega)$ should satisfy a homogeneity requirement. In a system of linear size L, one expects, over lengths much greater than the elastic scattering length, l_{elastic}, that L itself sets the unit of length. Correspondingly, over energies ω much less than the bandwidth, the mean level spacing, which is proportional to L^{-d}, sets the energy scale. Invariance under the scale change $L\to bL$ implies[1]

$$h(q,\omega)=b^d h(b^{-1}q,b^{-d}\omega)\equiv\hbar q^d f(q^d/\omega). \tag{1}$$

The new results presented in this paper are that, for electrons in the lowest Landau level with disorder, $f(q^2/\omega)$ has the form

$$f\left(\frac{q^2}{\omega}\right)=\begin{cases}D, & \text{if } q^2/\omega<c\rho(E_c),\\ [\omega c\rho(E_c)/q^2]^{\eta/2}D, & \text{if } q^2/\omega>c\rho(E_c),\end{cases} \tag{2}$$

for q,ω small. Estimated parameter values are given after Eq. (5). [Presumably there is a crossover region between the two limiting forms of Eq. (2), but apparent-

ly it is rather narrow.]

Thus an ω-independent characteristic length, $L_0 = [\omega c \rho(E_c)]^{-1/2}$, is generated, which can be interpreted as the size of a system having a mean level spacing at the mobility edge of order ω. Long-wavelength eigenfunction correlations, $\xi^{-1} < q < L_0^{-1}$, where ξ is the localization length, have the conventional, diffusive form, but at shorter wavelengths, $L_0^{-1} < q < l_{\text{elastic}}^{-1}$, correlations have the novel behavior $S(q;E_c,\omega) \propto \omega^{-\eta/2} q^{-2+\eta}$.

Our numerical calculations were motivated by recent analytical results.[4,5] First, a rigorous inequality for eigenfunction correlations in a single Landau level[4] excludes conventional, diffusive behavior for $S(q,\omega)$, but is consistent with the modified form we propose. (The correlation inequality *would* be satisfied with $\eta = 0$ *if* $\nu \lesssim \frac{1}{2}$, but this range for ν is ruled out by finite-size scaling calculations[6] and the Harris-Mott criterion.[7]) Second, perturbative calculations of quantum interference effects in high Landau levels,[5] analogous to weak-localization calculations in small magnetic field, reveal that the leading correction to diffusive behavior is a reduction in the diffusion constant at finite wave vector. This correction arises at first order in perturbation theory and therefore dominates over the universal reduction in dissipative conductivity found at second order. We interpret this result to indicate a crossover with increasing length scale from diffusive ($\eta = 0$) to critical ($\eta > 0$) correlations.

Our numerical results are for electrons in the lowest Landau level, moving in a Gaussian white-noise potential. We start from the Hamiltonian for noninteracting particles of mass m and charge $-|e|$ moving in the x-y plane with a uniform, perpendicular magnetic field of strength B and a potential $V(x,y)$:

$$H = (\hbar\omega_c/2)\{-l_c^2 \partial^2/\partial x^2 + (-l_c\,\partial/\partial y + x/l_c)^2\} + V(x,y) \equiv H_0 + V(x,y), \tag{3}$$

where $l_c^2 = \hbar/|e|B$ and $\omega_c = eB/m$. We treat a square system of side L and apply periodic boundary conditions in both directions, which requires $L^2 = 2\pi N l_c^2$, N integer. Eigenstates of H_0 from the lowest Landau level are then products of θ functions,[8] which are accurately approximated for the system sizes we study ($128 \le N \le 1024$) by

$$\langle x,y|m\rangle = \frac{(2N)^{1/4}}{L} \exp\left\{\frac{2\pi i m}{L}[y] - \frac{1}{2l_c^2}\left[x + \frac{mL}{N}\right]^2\right\},$$

for $m = 1,2,\ldots,N$, with $m + N \equiv m$, where square brackets indicate lengths measured modulo L, so that $-L/2 \le [x + mL/N] < L/2$ and $0 \le [y] < L$. In the strong-field limit, scattering between Landau levels may be neglected; the projection of Eq. (3) onto the lowest level is, after subtraction of zero-point energy,

$$\mathcal{H} = \sum_{m,m'=1}^{N} |m\rangle\langle m|V(x,y)|m'\rangle\langle m'|.$$

We take the potential, $V(x,y)$, to be essentially Gaussian white noise with zero mean and covariance

$$\langle V(x,y)V(x',y')\rangle = v^2 l_c^2 \delta(x-x')\delta(y-y').$$

More precisely, we take the Fourier components of $V(x,y)$ with wave vectors (k_x,k_y) for which $|k_x|$ or $|k_y| > 6.3 l_c^{-1}$ are omitted. Their contributions to the matrix elements of $\mathcal{H}$ are negligible, since the basis states are smooth functions.

We calculate $S(q;E_c,\omega)$ by numerically diagonalizing $\mathcal{H}$, assembling the eigenvectors and energies to form the spectral function, averaging over different realizations of the potential and, finally, extrapolating from a sequence of system sizes to obtain the large-N, small-q, small-ω limit.[9] If the eigenvector of $\mathcal{H}$ with energy E_α has expansion coefficients $a_\alpha(m)$ in the basis $\{|m\rangle\}$, let

$$Q_{\alpha\beta}(k,l) = N\left|\sum_{m=1}^{N} a_\alpha(m) a_\beta^*(m+l)\, e^{2\pi i k m/N}\right|^2,$$

with k,l integer. Then[4]

$$S(q;E,\omega) = (2\pi l_c^2 N^2)^{-1} e^{-q^2 l_c^2/2} \left\langle \sum_{\alpha,\beta} \delta(E - \omega/2 - E_\alpha)\delta(E + \omega/2 - E_\beta) Q_{\alpha\beta}(k,l)\right\rangle, \tag{4}$$

where $q^2 = 2\pi(k^2 + l^2)/N l_c^2$.

This expression is unsuitable for numerical evaluation because of the two δ functions. One is removed by integration on E over a narrow range around the mobility edge, and we replace the other with a sharply peaked weighting function. Thus we assume that $S(q;E,\omega)$ is independent of E over the range of energies for which the localization length in an infinite system is much larger than the size of our system. From the work of Aoki and Ando[6,10] we estimate this condition to be satisfied generously for the $2M$ eigenstates closest to $E = E_c \equiv 0$, if $M \le 0.35 N^{3/4}$. Equation (4) may then be replaced by

$$S(q;E,\omega) = 2\pi l_c^2 \rho^2(0) \exp(-q^2 l_c^2/2) K(q,\omega),$$

with

$$K(q,\omega) = \left\langle \sum_{\alpha,\beta}' w(\omega + E_\alpha - E_\beta) Q_{\alpha\beta}(k,l)\right\rangle \Big/ \left\langle \sum_{\alpha,\beta}' w(\omega + E_\alpha - E_\beta)\right\rangle, \tag{5}$$

where $\sum'_{\alpha,\beta}$ is the sum over the $2M$ states described above[11] and $w(\omega+E_\alpha-E_\beta)$ is chosen to be a Gaussian function with width σ of order the mean level spacing: $\sigma=\sigma_0/N$, $\sigma_0=0.64v$.

In this way we obtain $K(q,\omega)$ for $0\le k^2+l^2\le 19$ and $\omega=n\sigma$, $2\le n\le 19$ (k,l,n integer), where the upper limits are chosen so that $\omega\ll v$ and $q<l_c^{-1}$, even in the smallest systems studied. Averaging over 1000 realizations for $N=128$, 200 for $N=256$, 50 for $N=512$, and 10 for $N=1024$ resulted in statistical uncertainties of approximately 1% in $K(q,\omega)$.

We make the extrapolations $N\to\infty$ and $q,\omega\to 0$, with q^2/ω fixed, simultaneously as follows. If the scaling assumption, Eq. (1), is correct, then in these limits we expect

$$\omega K(q,\omega)=[2\pi^2 l_c^2\rho(0)]^{-1}[\hbar q^2 f(q^2/\omega)/\omega]/[1+\{\hbar q^2 f(q^2/\omega)/\omega\}^2],$$

which is a function only of the single variable q^2/ω. Each system size studied results in values for $\omega K(q,\omega)$ at twelve values of $q^2=2\pi(k^2+l^2)/Nl_c^2$, and eighteen values of $\omega=n\sigma_0/N$, producing 140 distinct values of q^2/ω. For each q^2/ω we combine data from all system sizes and extrapolate $\omega K(q,\omega)$ linearly in q^2 to $q=0$ and, by implication, $N=\infty$, $\omega=0$.[12] This extrapolation is illustrated in Fig. 1 for four representative q^2/ω values.

A preliminary examination of the extrapolated $\omega K(q,\omega)$, and hence $S(q;0,\omega)$, shows that a form similar to Eq. (2) is appropriate. Best values of $\rho(0)$, D, c, and η are obtained as follows. The $\omega K(q,\omega)$ values are divided into two sets: those for $q^2/\omega<a$ and those for $q^2/\omega>a$. The first set is fitted with $f(q^2/\omega)=D$ and the second set with $f(q^2/\omega)=(\omega a/q^2)^{\eta/2}D$, adjusting $\rho(0)$, D, a, and η. In this way we find $vl_c^2\rho(0)=0.149$, $\hbar D/vl_c^2=0.58$, $c\equiv a/\rho(0)\simeq 60$. The exponent lies in the range $\eta=0.38\pm 0.04$. Error estimates are problematic, both because of statistical correlations contained in $K(q,\omega)$ and because of uncertainty over systematic effects.

The value for $vl_c^2\rho(0)$ compares well with the known, exact result,[13] $\sqrt{2}/\pi^2\simeq 0.143$. The present value of the long-wavelength diffusion constant agrees reasonably well with a previous calculation[14] from a resummed perturbation series in v, of $\hbar D/vl_c^2=0.51$. At critical points in two-dimensional, statistical-mechanical systems, there is an established relation between η and a finite-size scaling amplitude.[15] If this relation also holds at a mobility edge, η can be found independently[16] from transfer matrix calculations of the localization length[16,17]; in fact, such estimates are $\simeq 30\%$ larger than the value given above.

A generalization of the functional form that we fitted is obtained by allowing a second exponent, $\eta'\neq 0$, for $q^2/\omega<a$. From this we obtain $\eta'=0.064$, with little change in η. Since the zero-temperature, dc dissipative conductivity is proportional to $f(0)$, $\eta'\equiv 0$ is clearly preferred.

The behavior of $f(q^2/\omega)$ is shown in Fig. 2. The collapse of the data onto a single curve is strong support for the scaling assumption, Eq. (1). It is clear that eigenfunction correlations near the mobility edge, and on length scales between the magnetic length and the localization length, cannot be characterized solely by a diffusion constant; instead they are well represented by Eq. (2).

Our results give no direct insight into the reason for the divergence of the localization length at the Landau band center. However, we feel that a complete theory of localization in the integer quantum Hall regime should

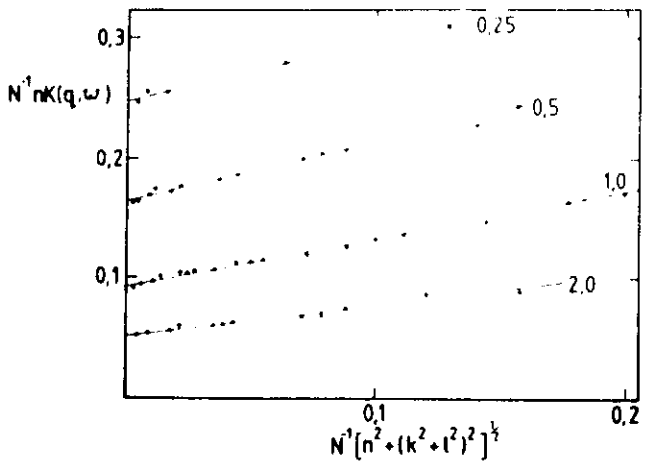

FIG. 1. Illustration of extrapolation of $K(q,\omega)$ to $N=\infty$, $q^2=\omega=0$ with q^2/ω fixed. For clarity, only a representative selection of data points are shown. Lines are labeled with values of $(k^2+l^2)/n$.

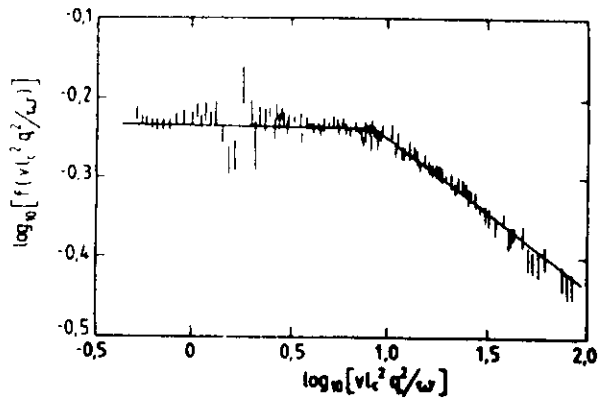

FIG. 2. Fit of extrapolated data (points with estimated errors) by Eq. (2) (line), for parameter values given in text. A representative selection of the 140 data points is shown. The large errors near $\log_{10}(vl_c^2q^2/\omega)=-0.2$ reflect the intrinsic difficulty in our obtaining $f(q^2/\omega)$ from $S(q,\omega)$ near the maximum in $S(q,\omega)$. Units of f are $vl_c^2/\hbar$.

include predictions of the scaling form Eq. (2), for eigenfunction correlations on scales shorter than the localization length. The behavior we find for small q^2/ω is compatible with the field theory proposed by Pruisken and co-workers[2]; the anomalous correlations at large q^2/ω may have an instanton interpretation in that context.

A direct experimental test of the scaling form is likely to be difficult because the obvious measurement, conductivity, probes $q=0$. An indirect signature should appear in the temperature dependence of the inelastic scattering rate, and hence the peak values of the dissipative conductivity between Hall plateaus, because the spatial overlap of eigenfunctions close in energy is large:

$$\langle |\psi_\alpha(\mathbf{r})\psi_\beta(\mathbf{r})|^2\rangle \sim |E_\alpha - E_\beta|^{-\eta/2}$$

for E_α, E_β near E_c. In theoretical terms, the consequence of the eigenfunction correlations we find is that a wave packet spreads with (diameter)$^2 \propto$ time, because the scaling variable is q^2/ω, but the wave packet never approaches the Gaussian asymptotic form reached by solutions to the diffusion equation. Clearly, the nonzero value of η may be a consequence of fractal structure in eigenfunctions.[18]

It is natural to ask whether similar correlations are likely to occur near the mobility edge in other systems. An obvious candidate is the localization transition in two dimensions that occurs when spin-orbit scattering is strong.

In summary, we have shown that eigenfunction correlations have novel scaling behavior near the mobility edge in a model for the integer quantum Hall effect.

We wish to thank Paolo Carra for previous collaborations and many discussions, from which the present work originated.

[1]P. A. Lee and T. V. Ramakrishnan, Rev. Mod. Phys. 57, 287 (1985); F. Wegner, Z. Phys. B 25, 327 (1976); Y. Imry, Y. Gefen, and D. J. Bergman, Phys. Rev. B 26, 3436 (1982); E. Abrahams and P. A. Lee, Phys. Rev. B 33, 683 (1986).

[2]H. Levine, S. B. Libby, and A. M. M. Pruisken, Phys. Rev. Lett. 51, 1915 (1983); A. M. M. Pruisken, in *The Quantum Hall Effect*, edited by R. E. Prange and S. M. Girvin (Springer-Verlag, New York, 1987).

[3]B. Velicky, Phys. Rev. **184**, 614 (1969).

[4]J. T. Chalker, J. Phys. C **20**, L493 (1987).

[5]J. T. Chalker, P. Carra, and K. A. Benedict, Europhys. Lett. 5, 163 (1988).

[6]H. Aoki and T. Ando, Phys. Rev. Lett. **54**, 831 (1985).

[7]A. B. Harris, J. Phys. C 7, 1671 (1974); N. F. Mott, Philos. Mag. B **44**, 265 (1981); J. T. Chayes, L. Chayes, D. S. Fisher, and T. Spencer, Phys. Rev. Lett. **57**, 2999 (1986).

[8]F. D. M. Haldane and E. H. Rezayi, Phys. Rev. B **31**, 2529 (1985).

[9]Diagonalization of a square system is a suitable technique because we are interested in properties on scales short compared with the (divergent) localization length; to determine the localization length itself, finite-size scaling calculations on long strips (Ref. 6 and references therein) would of course be more appropriate. Matrix diagonalization used routines supplied by the Nottingham algorithms group.

[10]The authors of Ref. 6 use for the potential $V(x,y)$ a high concentration of mixed repulsive and attractive short-range scatterers, which is distinct from, but close to, our choice of Gaussian white noise.

[11]We omit diagonal terms, $\alpha=\beta$, from the sums in Eq. (5), which would otherwise make a small contribution to $K(q,\omega)$ via the tails of $w(\omega+E_\alpha-E_\beta)$. This is done because the orthogonality of eigenstates results in behavior for $Q_{\alpha\alpha}(k,l)$ different from that for $Q_{\alpha\beta}(k,l)$, $\alpha\neq\beta$.

[12]The physical limit is actually *first* $N\to\infty$, *then* $q^2,\omega\to 0$. It is not feasible to reach the regime $l_c^{-1}\gg q\gg L^{-1}$ with the present technique. If results did depend on the value of Lq, points in Fig. 1 would not like on single curves for each value of q^2/ω.

[13]F. Wegner, Z. Phys. B **51**, 279 (1983).

[14]R. Singh and S. Chakravarty, Nucl. Phys. **B265 [FS15]**, 265 (1986).

[15]J. L. Cardy, J. Phys. A **17**, L385 (1984).

[16]J. L. Pichard and G. Sarma, J. Phys. C **14**, L127 (1981); J. T. Chalker, J. Phys. C **21**, L119 (1988).

[17]J. T. Chalker and P. D. Coddington, J. Phys. C **21**, 2665 (1988).

[18]H. Aoki, J. Phys. C **16**, L205 (1983).